Carbohydrate Polymers, vol. 251, 2021, pp. 11705-5.

Polysaccharide-based triboelectric nanogenerators: A review.

Torres, Fernando G. y De-la-Torre, Gabriel Enrique.

Carbohydrate Polymers 251 (2021) 117055

Contents lists available at ScienceDirect

Carbohydrate Polymers

journal homepage: www.elsevier.com/locate/carbpol

Review

Polysaccharide-based triboelectric nanogenerators: A review

Fernando G. Torres [a,*], Gabriel E. De-la-Torre [b]

[a] Department of Mechanical Engineering, Pontificia Universidad Catolica del Peru, Av. Universitaria 1801, 15088, Lima, Peru
[b] Universidad San Ignacio de Loyola, Av. La Fontana 501, Lima 12, Lima, Peru

ARTICLE INFO

Keywords:
Triboelectric nanogenerators (TENGs)
Green electronics
Recyclable electronics
Biopolymer
Cellulose
Chitosan
Starch

ABSTRACT

Triboelectric nanogenerators (TENGs) are versatile electronic devices used for environmental energy harvesting and self-powered electronics with a wide range of potential applications. The rapid development of TENGs has caused great concern regarding the environmental impacts of conventional electronic devices. Under this context, researching alternatives to synthetic and toxic materials in electronics are of major significance. In this review, we focused on TENGs based on natural polysaccharide materials. Firstly, a general overview of the working mechanisms and materials for high-performance TENGs were summarized and discussed. Then, the recent progress of polysaccharide-based TENGs along with their potential applications reported in the literature from 2015 to 2020 was reviewed. Here, we aimed to present polysaccharide polymers as a promising and viable alternative to the development of green TENGs and tackle the challenges of recycling e-wastes.

1. Introduction

In recent years, significant efforts have been devoted to the developing of next generation electronics with versatile characteristics for a wide range of applications. The development of smart devices focused on wearable, wireless, portable, self-charging, cost-efficient and even implantable electronic equipment. Under this context, simple and durable ambient energy harvesting devices are needed to overcome conventional and unsustainable power supply limitations (Zhu, Peng, Chen, Jing, & Wang, 2014). In particular, mechanical energy found in the environment can be used to generate electric energy exploiting electrostatic (Boisseau, Despesse, & Ahmed, 2012), electromagnetic (Yang et al., 2009), piezoelectric (Narita & Fox, 2018) and triboelectric effects (Tian, Chen, & Wang, 2020). Among them, piezoelectric nanogenerators (PENGs) and triboelectric nanogenerators (TENGs) feature more significant potential applications.

Piezoelectric materials undergo a change in polarization when they are subjected to mechanical deformation (strain) (Nye, 1957). Ceramics, such as zirconate titanate (Pb(Zr1–X, TiX)O3, known as PZT) and barium titanate ($BaTiO_3$) were the first materials used to develop piezoelectric generators. However, ceramics usually feature inherent mechanical brittleness that prevents them from being used for modern applications that need more flexible materials (Mangayil et al., 2017). In order to overcome such limitations, synthetic and biodegradable polymers, as well as polymeric composites have been used to develop PENGs (Sun, Zeng, & Li, 2020). For instance, polysaccharides, such as chitosan (Hänninen, Rajala, Salpavaara, Kellomäki, & Tuukkanen, 2016, 2018), cellulose (Rajala et al., 2016; Sriplai et al., 2020; Tuukkanen & Rajala, 2018) and bacterial cellulose (Mangayil et al., 2017) have been reported to be used as lightweight and flexible piezoelectric materials. However, PENGs are known to be efficient when the frequency of the mechanical excitation ranges 60−100 Hz (Han et al., 2013; Liu, Zhong, Lee, Lee, & Lin, 2018). For lower frequencies, extremely low voltage values are obtained by PENGs.

On the other hand, TENGs have been used to harvest energy from low frequency sources (around 10 Hz and lower) such as human body motion, animal organs, and water motion, among others (Gong et al., 2019; Zhou, Liu, Wang, & Wang, 2020). The working principle of these TENGs is a combination of the triboelectric effect and the electrostatic induction (Fan, Tian, & Wang, 2012). The triboelectric effect, also known as contact electrification, takes place when two materials are brought into contact and then separated. According to the "Surface state model", when two different surfaces are contacted, electrons attempt to transfer from the surface of higher Fermi level to the surface of lower Fermi level (Harper, 1957). This phenomenon is far from being completely elucidated and the characteristics of the proposed mechanisms remain highly debated (Wang, Xie, Niu, Lin, Liu et al., 2014). TENGs are designed to alternatively contact and separate two materials having opposite triboelectric polarities in order to alternately drive induced electrons to flow between the electrodes (Ghosh et al., 2008).

* Corresponding author.
E-mail address: fgtorres@pucp.pe (F.G. Torres).

https://doi.org/10.1016/j.carbpol.2020.117055
Received 23 July 2020; Received in revised form 13 August 2020; Accepted 2 September 2020
Available online 11 September 2020

The voltage and the current outputs of TENGs are proportional to the triboelectric charge density on the surface, and the output power has a quadratic dependence on the charge density (Niu, Liu et al., 2013, 2013b). TENGs present a promising alternative for efficient environmental, biomechanical energy harvesting and self-powered pressure, vibration, motion and chemical sensing (Ma et al., 2018).

Important progress has been made on the development of novel highly efficient TENGs with interesting characteristics since it was first described in 2012 by Wang's group.

TENGs are suggested to be part of the rapid development of an Internet of Things (IoT) era due to an increased interest in self-powered applications (Shi & Wu, 2019). However, there has been a major concern over the environmental impact that the production of futuristic electronics may cause. Electronic products are complicated to recycle once they reach their end-of-life due to the many different integrated materials and components (Tanskanen, 2013). Many TENGs are based on synthetic polymers, like polytetrafluoroethylene (PTFE), polyvinylidene fluoride (PVDF) or polyethylene terephthalate (PET), with stable chemical bonding (Zhang, Tang et al., 2019, 2016; Zhao, Pu et al., 2016), resulting in decades-long environmental degradation and the release of toxic chemicals. Moreover, the large accumulation of electronic waste (e-waste) may pose environmental and health risks in urban areas (Needhidasan, Samuel, & Chidambaram, 2014). Hence, academic research on eco-friendly and highly degradable materials for TENG development has become of great significance (Li et al., 2020).

Polysaccharides are biopolymers consisting of monosaccharides linked through glycosidic bonds. They are essential biological macromolecules in nature and found widespread in plants, seaweed, fungi and microorganisms (Zong, Cao, & Wang, 2012). Many researchers have investigated the application of various polysaccharides as the main component of modern green electronics (Kumar, Ranwa, & Kumar, 2020; Kwon et al., 2018; Miao, Liu, Li, & Zhang, 2018; Zhao et al., 2020), including TENGs.

Several recent reviews are focused on the materials used to develop TENGs. For instance, Chen et al. (2020) reviewed the polymer materials for high-performance TENGs, focusing on the ones that are most frequently adopted. Among these, cellulose-based TENGs are reviewed and other polysaccharide-based materials are rapidly mentioned. Yu, Zhu, Wang, and Zhai (2019) summarized the materials engineering techniques, either physical or chemical, for high-performance TENGs. Maiti, Karan, Kim, and Khatua (2019) focused on biodegradable/biocompatible materials for PENGs and TENGs. Some polysaccharide-based TENGs are described in detail, although the broad scope of the review overlooked many high-performance polysaccharide-based TENGs developed recently. The number of published articles on polysaccharide-based TENGs has increased significantly in recent years. However, no previous review has focused on this specific type of materials. Hence, in this review we cover the recent progress of TENGs based on natural polysaccharides as reported in the literature. A general overview of TENGs and their working mechanisms were summarized, as well as the polysaccharide materials aspects allowing the development of novel, high-performance and eco-friendly TENGs. Then, the available literature regarding the development and appliances of polysaccharide-based TENGs were reviewed. Lastly, the general challenges and future perspectives were discussed. We aim to provide guidance across new sustainable and biodegradable materials for the development of TENGs as a promising breakthrough for facing the challenges of recycling electronics and minimizing environmental impacts.

2. An overview of triboelectric nanogenerators

2.1. Working mechanism

The first TENG, developed by the Wang group consisted of two polymer films, Kapton (125 μm in thickness) and polyester (PET, 220 μm in thickness), sandwiched together and covered with thin layers of Au alloy films that served as electrodes (Fan et al., 2012). After the two polymer materials come into contact due to bending or mechanical compression, surface electric charges are induced, creating a triboelectric potential layer between the two polymers. Upon release, the Au alloy electrodes build electric potential difference, resulting in current flow if connected to an external load as described in Fig. 1. When the two surfaces coming into contact again under mechanical stimuli, a change in the potential difference on the electrodes is observed and current flows back in the opposite direction. By constantly repeating the described cycle, a continuous AC output is obtained (Wu, Wang, Ding, Guo, & Wang, 2019). Since it was first developed in 2012, a broad range of materials, working models and applications have been developed and proposed in the literature, which looks to inspiring an energy and sensors revolution (Khandelwal, Maria Joseph Raj, & Kim, 2020; Kim, Lee, Kim, & Jeong, 2020; Wang, 2020a; Zhou et al., 2020).

2.2. Working modes

From the development of the first TENG, four working modes have been developed based on the same fundamental principle: Vertical contact-separation mode, lateral-sliding mode, single-electrode mode, and freestanding triboelectric-layer mode (Wang, 2014).

The vertical contact-separation mode (Fig. 2a) is the earliest working mode as described above. In brief, two different dielectric materials are stacked and a metal layer that serves as an electrode is deposited on the surfaces of both materials. The contact and release of both oppositely charged surfaces due to displacement by an external mechanical stimuli causes the induced potential to change across the electrodes (Wang, Lin, & Wang, 2012; Zhu et al., 2012). In a later mode consisting of a single dielectric layer and two electrodes, the electrode coming into contact with the dielectric layer plays the role of generating triboelectric charges and transferring chargers between electrodes (Niu, Wang et al., 2013). The theoretical study of both dielectric-dielectric and dielectric-conductor modes have been described by Niu, Liu et al. (2013, 2013b).

With a similar setup to the vertical contact-separation mode, the contact-sliding mode (Fig. 2b) consists of the in-plane sliding friction between the two dielectric materials, causing intensive triboelectrification on the surfaces. These contact changes between surfaces give rise to a separation in charge centers, leading to a voltage drop for driving the flow of electrons in an external load (Lin et al., 2013; Wang et al., 2013). This principle allows for harvesting mechanical energy from a variety of planar surfaces, including rotational motion (Zhu, Chen et al., 2013). The theoretical basis of the lateral-sliding mode was developed by Niu, Liu et al. (2013).

The single-electrode mode (Fig. 2c) consists of only one electrode connected to ground that comes into contact with a single dielectric layer, rather than a sandwich-like mode as aforementioned. Based on the same principals as previous modes, the change in contact between the dielectric layer and electrode induces a charge transfer between the electrode and ground and across an external load (Yang, Zhang et al., 2013, 2013b). This mode allows to harvest mechanical energy from systems that cannot move freely but are static or grounded (Wang, 2014). Theoretical research and structural optimization of single-electrode TENGs was developed by Niu et al. (2014).

Lastly, the freestanding triboelectric-layer mode (Fig. 2d) is based on the triboelectric effect between a sliding dielectric layer and two electrodes connected to a load (Wang, Lin, Chen, Niu, & Zi, 2016). The first paper to describe this mode developed three types: Dielectric-to-conductor in contact sliding mode, dielectric-to-conductor in non-contact sliding mode and dielectric-to-dielectric mode (Wang, Xie, Niu, Lin, & Wang, 2014). In the dielectric-to-conductor in contact sliding mode, two stationary electrodes are placed separated by an in-plane distance and a dielectric layer comes into contact and slides forward and backwards from the first electrode to the second,

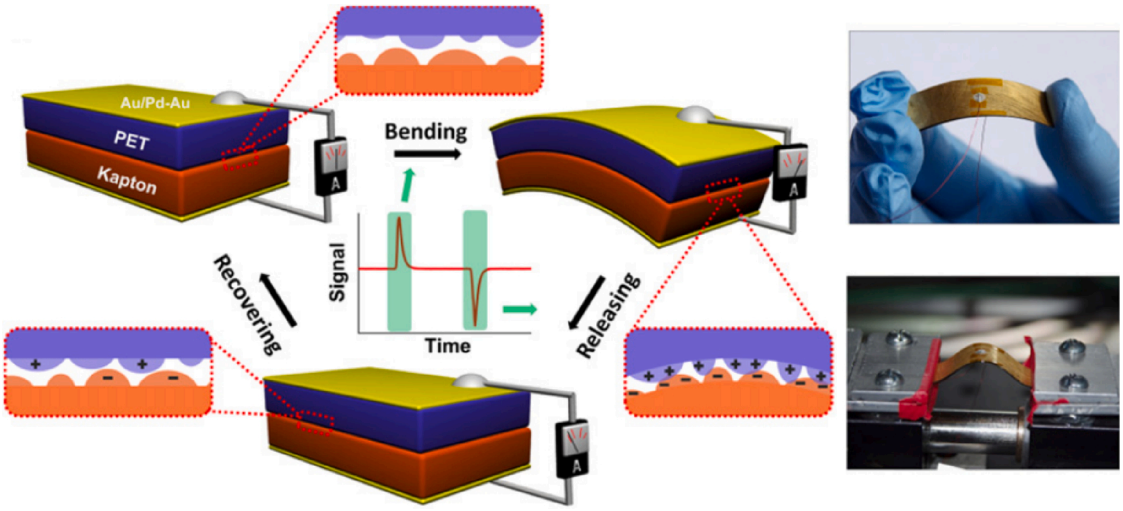

Fig. 1. Schematic and photos of the working mechanism of the first triboelectric nanogenerator. Reprinted from (Fan et al., 2012). Copyright (2012) with permission from Elsevier.

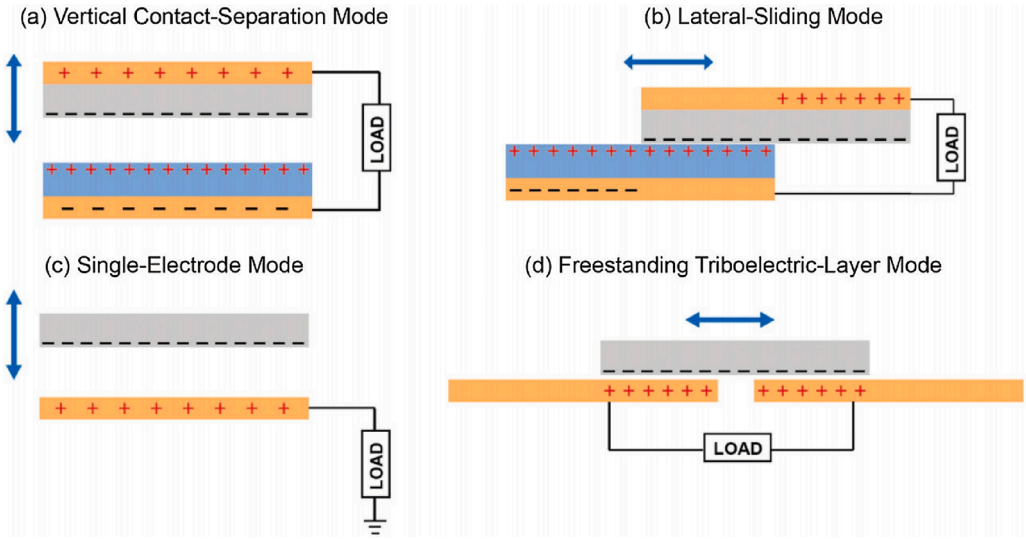

Fig. 2. Schematic representations of the four working modes. Electrodes (conductors) are orange, dielectric materials are grey (-) and blue (+). a) Vertical contact-separation mode; b) lateral-sliding mode; c) single-electrode mode; d) freestanding triboelectric-layer mode. Reprinted from (Wu et al., 2019). Copyright (2019) with permission from Wiley-VCH. (For interpretation of the references to colour in this figure legend, the reader is referred to the web version of this article.).

generating triboelectric charges, while in the non-contact sliding mode the dielectric layer slides without direct contact with the electrodes. Lastly, the dielectric-to-dielectric mode consists of the same structure as the previous freestanding modes but including a positively charged dielectric layer covering the two stationary electrodes, where the negatively charged dielectric layer slides in contact with the second dielectric layer. Accordingly, the theoretical bases are described by Niu et al. (2015).

Table 1 shows a list of the most recent polysaccharide-based TENGs reported. Most of these TENGs are arranged using the vertical contact separation mode (VCS). Few studies report the single-electrode mode. In these modes, the electricity is generated through an alternative normal contact and separation of the working surfaces. These modes are the most widely used, probably due to their simple structural design, compared to the other two working modes (i.e. lateral sliding and freestanding modes) which need an in-plane sliding between two surfaces in lateral direction (10.1021/nl400738p).

3. Materials science aspects of high-performance TENGs

Any pair of materials with different charges can be used for assembling a TENG (Wu et al., 2019). However, the performance of TENGs depends on the surface structure, triboelectric surface charge density, dielectric property and material robustness (Chen, Zhang, Zhu, & Wang, 2020). This makes the choice of materials a crucial step in developing TENGs. For instance, triboelectric series, a material rank according to their electron-gain or -withdrawal trend, may be helpful for the choice of materials (Zou et al., 2019). Larger differences in triboelectric charge density (far apart from each other in the triboelectric series) between two rubbing materials will be translated into greater transferred charges (Lee et al., 2019).

Polysaccharides have been included in triboelectric series with minor discrepancies across authors (An, Sankaran, & Yarin, 2018; Diaz & Felix-Navarro, 2004). Cellulose derived compounds with triboelectric charge densities similar to common synthetic polymers could serve as potential substitutes. Importantly, functional groups are associated with enhancing the electron-gaining or -withdrawal nature of biopolymers.

Table 1
Summary of the electrical performance of polysaccharide-based TENGs in the literature. VCS: Vertical contact-separation mode. SE: Single-electrode mode. V_{OC}: Open-circuit voltage output. I_{SC}: Short-circuit current output.

Working mode	Materials	V_{OC}	I_{SC}	Power density	Reference.
VCS	Bacterial nanocellulose Cu electrodes	13 V	~3 μA	4.8 mW m^{-2}	(Kim, Yim et al., 2017)
VCS	BC + $BaTiO_3$ PDMS Cu electrodes	181 V	21 μA	4.8 mW m^{-2}	(Shao et al., 2019)
VCS	BC + $BaTiO_3$ + Ag NW PTFE Al electrode	170 V	9.8 μA	180 μW cm^{-2}	(Oh et al., 2019)
SE	BC + ZnO Teflon ITO electrode	49.6 V	4.9 μA	–	(Jakmuangpak et al., 2020)
VCS	Cellulose/ PDMS Al electrodes	28 V	2.8 μA	64 μW cm^{-2}	(Chandrasekhar et al., 2017)
VCS	NCC-filled PDMS Al electrodes	320 V	–	0.76 mW cm^{-2}	(Peng et al., 2017)
Corrugated core	PET/Al/PI core MCC/Al plates	153 V	3.9 μA	–	(Uddin & Chung, 2017)
VCS	CMF/CNF/Ag FEP	21.9 V	0.17 μA	7.68 μW cm^{-2}	(He et al., 2018)
VCS	Allicin-grafted CNF PVDF Electrodes	7.9 V	5.13 μA	10.13 μW cm^{-2}	(Roy et al., 2020)
Gear-like VCS	CNF-PEI-Ag FEP Cu electrodes	286 V	4 μA	0.43 W m^{-2}	(Zhang, Lin et al., 2019)
VCS	AZO-coated CNF AZO-coated CNF + $TiCl_4$	7 V	0.7 μA	–	(Yang et al., 2017)
VCS	CNF/ phosphorene Au electrodes	5.2 V	–	9.36 μW cm^{-2}	(Cui et al., 2017)
VCS	CNF film FEP ITO/PET substrate/ electrode	32.8 V	35 μA	–	(Yao, Hernandez, Yu, Cai, & Wang, 2016)
VCS	CA-PEI LTV Conductive fabric	478 V	–	2.21 mW cm^{-2}	(Bai et al., 2020)
VCS	CA PTFE Al electrodes	7.3 V	9.1 μA	–	(Srither et al., 2018)
VCS	EC 317 L SS Ag electrode	245 V	50 μA	–	(Wang et al., 2017)
VCS	EC	45 V	–		

Table 1 (*continued*)

Working mode	Materials	V_{OC}	I_{SC}	Power density	Reference.
				1.2 mW m^{-2}	(Šutka et al., 2018)
VCS	PDMS PCL/GO	120 V	4 μA	72.5 mW m^{-2}	(Parandeh et al., 2019)
VCS	Cellulose paper Au electrodes Crepe paper	196.8 V	31.5 μA	16.1 W m^{-2}	(Chen et al., 2019)
VCS	Nitrocellulose membrane Cu electrodes PPy-coated cellulose paper	60 V	8.8 μA	0.83 W m^{-2}	(Shi, Chen et al., 2019)
VCS	Cellulose paper Nitrocellulose membrane CNF aerogel	55 V	0.94 μA	29 mW m^{-2}	(Qian et al., 2019)
VCS	PDMS Ag electrodes Cellulose II aerogel	65 V	1.86 μA	127 mW m^{-2}	(Zhang et al., 2020)
VCS	PTFE Al electrodes Cellulose II/ chitosan aerogel	242 V	–	–	(Zhang et al., 2020)
VCS	PTFE Al electrodes Cellulose II/ alginic acid aerogel	~80V	–	–	(Zhang et al., 2020)
VCS	PTFE Al electrodes CMC aerogel/ PDMS	~14 V	~0.22 μA	–	(Beyranvand & Gholizadeh, 2020)
VCS	PDMS Kapton Al electrodes Cellulose/ $BaTiO_3$ aerogel PDMS	48 V	–	–	(Shi, Huang et al., 2019)
VCS	Al electrodes CNF/PEI aerogel PVDF nanofibers	106.2 V	9.2 μA	13.3 W m^{-2}	(Mi et al., 2018)
VCS	Al electrodes Wood	220 V	5.8 μA	158.2 mW m^{-2}	(Hao et al., 2020)
VCS	PTFE Cu electrode Wood	81 V	1.8 μA	57 mW m^{-2}	(Luo et al., 2019)
VCS	PTFE Cu electrodes Chitosan-glycerol film	130 V	~15 μA	–	(Jao et al., 2018)
VCS	PTFE Al electrode Chitosan-acetic acid	~1.6 V	~40 nA	17.5 μW m^{-2}	(Wang et al., 2018)
VCS	Kapton Al electrode Chitosan aerogel PI ITO	60.6 V	7.7 μA	2.33 W m^{-2}	(Zheng et al., 2018)

(*continued on next page*)

Table 1 (*continued*)

Working mode	Materials	V_{OC}	I_{SC}	Power density	Reference.
VCS	Chitosan-diatom film FEP Al electrodes	150 V	1.02 μA	15.7 mW m^{-2}	(Kim, Lee, Go et al., 2020)
SE	Chitosan hydrogel + Ag NW + Cu^{2+} PDMS	218 V	–	2 W m^{-2}	(Wang & Daoud, 2019)
VCS	Chitosan film PDMS Al electrodes	306 V	–	–	(Yu et al., 2020)
VCS	Starch film Mixed cellulose ester Cu electrodes	300 mV	–	–	(Ccorahua, Cordero et al., 2019)
VCS	Starch film + $CaCl_2$ PTFE Al electrodes	1.2 V	–	170 mW m^{-2}	(Ccorahua, Huaroto et al., 2019)
VCS	thermoplastic starch PDMS Carbon tape electrodes	~560 V	0.18 mA	17 W m^{-2}	(Sarkar et al., 2019)
SE	Starch paper Wire electrode	~14 V	–	–	(Zhu et al., 2018)
VCS	Calcium alginate film Al electrodes	33 V	150 nA	–	(Pang et al., 2018)
VCS	Sodium alginate PVA Li and Al electrodes	1.47 V	3.9 nA	3.8 mW m^{-2}	(Liang et al., 2017)
Cased	Alginate/PVA hydrogel + $CaCl_2$ + borax PDMS bag Al electrode	203.4 V	17.6 μA	0.98 W m^{-2}	(Jing et al., 2020)
VCS	Pullulan + NaF film Kapton Ag and Al electrodes	79 V	–	41.1 mW m^{-2}	(Lu et al., 2020)

For instance, Ma et al. (2019) associated the reduced electrical performance of chitosan dissolved in citric acid TENG after reaching 1:6 (chitosan: citric acid) mass ratio to the decrease of the electron-donating amino and hydroxyl groups revealed by FTIR spectra. Surface-charge engineering allows to increase or decrease the triboelectric charge density by changing the end-functional groups on the friction layers (Song et al., 2015; Wei, Zhu, & Wang, 2014). For instance, the tribopolarity of cellulose can be changed by attaching different functional groups depending on their electron-giving or -withdrawal nature. For example, nitro and methyl groups attached to CNF to control its surface charge (Yao, Yin, Yu, Cai, & Wang, 2017). A clear example is reported by Yao et al. (2017), where surface charge density of pristine cellulose nanofiber (CNF) films was -13.3 μC m^{-2}, while nitro-CNF and methyl-CNF resulted in 85.8 μC m^{-2} and -62.5 μC m^{-2} respectively. This process enables the development of highly efficient all-polysaccharide TENGs undergoing simple chemical procedures (Chen, Jiang, Xu, & Gong, 2019).

Surface morphology is another significant variable in a TENG performance. Studies have stated that larger TENGs (larger contact areas) will deliver higher outputs due to the increase of total transferred charges (Lee et al., 2019). The total contact area can be optimized by increasing the surface roughness in the friction layers (Vivekananthan, Chandrasekhar, Alluri, Purusothaman, & Kim, 2020). To address this issue, many techniques have been reported in the literature, like sandpaper treatment (Zhao, Zheng et al., 2016), hot embossing (Saadatnia, Esmailzadeh, & Naguib, 2019), electrospun fiber deposition (Pan et al., 2018), plasma etching (Kim, Kim, Kwon, Jo, & Kim, 2017), cold compression (Sriphan & Vittayakorn, 2018) ultrafast laser or added metallic nanowires (Lee et al., 2019). These methods are not exclusive to synthetic polymer-based TENGs. For example, Ccorahua, Huaroto, Luyo, Quintana, and Vela (2019) used sandpaper as a substrate for casting starch films with rough surfaces. Inductively coupled plasma has effectively enhanced the performance of an ethyl cellulose-based TENG (Wang et al., 2017). Alternatively, nanostructures can be introduced into the contact materials, creating nanocomposites with enhanced triboelectrification and conductivity (Wang, 2013). For instance, Kim, Jeon, Kim, You, and Kim (2018) conducted a filtration process to insert silver nanowires into a cellulose nanofiber paper that was utilized as both dielectric layer and electrode. Surface roughness must come hand in hand with surface robustness (Wang, 2020b). A surface that is too rough could deteriorate with usage, reducing the lifetime of the TENG (Chen et al., 2020). Cellulose has proved to be robust enough to withstand thousands of cycles and weathering conditions without diminishing their electrical performance (Bai et al., 2020; Chen et al., 2019).

Some polysaccharide comes with built-in micro- and nanostructures, mostly fibrils. Various derivatives of cellulose consist of nanofiber networks (e.g., bacterial cellulose, nanocrystalline cellulose, nanofibrillated cellulose) that increase the surface roughness of the material. Researchers have taken advantage of these characteristics to fabricate rough-surface and highly porous polysaccharide-TENGs (Jung et al., 2015; Kim, Yim et al., 2017; Šutka et al., 2018).

Many toxics, non-degradable and inorganic compounds are widely used in smart electronics, compromising environmental safety and human health (Maiti et al., 2019). The most remarkable characteristics of polysaccharide-based TENGs are the biodegradability, recyclability and minimum environmental impact. Lu, Li, Ping, He, and Wu (2020) fabricated a pullulan-based film for TENG applications that is fully recyclable while maintaining its performance after reuse. Liang et al. (2017) developed a sodium alginate-based TENG that dissolves in water entirely, including the electrodes, based on cascade chemical reactions without release trace toxic chemicals. The importance of biodegradability and biocompatibility for biomedical application will be further discussed in Section 5.3.

Another important characteristic of polysaccharides is their hydrophilic nature. Hydrophilic surfaces are usually regarded as not suitable for TENGs as they readily absorb moisture from the air and a thin monolayer of water molecule might spread over the surface. The presence of water molecules hinders the charge transfer between the two surfaces and leads to a decrease in triboelectrification (Li, Shen, Abdalla, Yu, & Ding, 2017). The decrease in the electric output is due to the fact that the charge transfer follows an electron pathway. It has been shown that the transferred charges during triboelectrification could be either electrons or ions (Lacks & Mohan Sankaran, 2011; McCarty & Whitesides, 2008). Thus, TENGs can be designed to have mobile ions as additional charges in the triboelectric layers (Chang et al., 2016). Wang et al. (2018) prepared chitosan-glycerol TENGs for energy harvesting. They found that the presence of glycerol increases the absorption of water from the air onto the film surface, enabling the channels of mobile ions for more efficient transfer of induced triboelectrification charges.

All in all, polysaccharide materials are suitable for TENG development. It has been demonstrated that their triboelectric charges are similar to that of some synthetic polymers (An et al., 2018; Diaz & Felix-Navarro, 2004). Additionally, polysaccharide materials are compatible with functional group change procedures and surface morphology engineering. These two aspects are important to the

development of high-performance TENGs. Furthermore, these biopolymers exhibit excellent degradation, low toxicity and cost-efficiency. Hence, polysaccharide-based polymers present a promising alternative for future green electronics.

4. Polysaccharide materials used for TENGs

In order to tackle the environmental problems caused by non-biodegradable and toxic materials commonly found in electronics, the development of eco-friendly biopolymer-based devices is of major concern to the scientific community (Li et al., 2020). Polysaccharides are key biopolymers for electronic appliances, some applications are memory devices (Hosseini & Lee, 2015), sensors (Sadasivuni et al., 2015), transistor-energy devices (Li et al., 2016), polymer electrolytes (Torres, Arroyo, Alvarez et al., 2019; Torres, Arroyo, & Troncoso, 2019) and photocatalytic H_2 production (Ke et al., 2009). In this section, the development of a variety of polysaccharide-based TENGs, namely cellulose, chitosan, starch, alginate and pullulan, described in the literature are reviewed. The overall summary of the polysaccharide-based TENGs and their electrical performance is shown in Table 1.

4.1. Cellulose

4.1.1. Bacterial cellulose

Bacterial cellulose (BC) is a versatile material produced by some types of bacterial (Wang, Tavakoli, & Tang, 2019). BC is composed of different types of nanofiber networks of 20−100 nm in diameter (Klemm et al., 2011) with remarkable mechanical properties and a wide range of applications (Torres, Arroyo, Alvarez et al., 2019, 2019b). Some studies were able to take advantage of these properties for the development of BC-based TENGs. Kim, Yim et al. (2017) produced BC following standard procedures (Jeon, Oh, Kee, & Kim, 2010) subsequently made a uniform bacterial nanocellulose (BNC) film by dissolving the BC in ethyl acetate and employing ultra-sonication for homogenization before casting on a copper foil. For the fabrication of a BNC-based TENG, the BNC cast on copper foil served as the top layer, while a secondary foil fixed on a flat polyoxymethylene plate as both electrode and a dielectric layer. They developed a second TENG deemed as a reference by adding a layer of polyimide (PI), a commonly used dielectric material in TENGs, as the second dielectric. The open-circuit output peak values of both BNC-based and reference TENGs were 13 V and 7 V, respectively. Jakmuangpak, Prada, Mongkolthanaruk, Harnchana, and Pinitsoontorn (2020) developed a BC film with ZnO nanoparticles that increased the surface roughness and polarizability. The BC film was assembled with Teflon and ITO glass layers for the fabrication of a single-electrode TENG, which exhibited 49.6 V and 4.9 μA of open-circuit voltage and short-circuit current.

Shao, ping Feng, wen Deng, Yin, and bo Yang (2019) developed a TENG based on BC nanofiber/$BaTiO_3$ composite film and PDMS as a dielectric. The $BaTiO_3$ nanoparticles allowed for an increased roughness of the film. The optimum volume ration of $BaTiO_3$ (13.5 vol%) reached 181 V of open-circuit output voltage and 21 μA short-circuit current. BaTiO3 significantly enhanced the TENG performance, as the reference BNC-based TENG achieved up to 120 V and 9.7 μA, thus elucidating a novel method for increasing triboelectric potential. Oh et al. (2019) developed a ferroelectric cellulose composite paper containing silver nanowires and $BaTiO_3$ within a BC matrix. The composite paper served as a positive triboelectric layer and electrode as it exhibits high electrical conductivity. In order to enhance the triboelectric potential, the dipoles in the BC composite were aligned through a poling process consisting of a sandwich-like setup of nylon films and aluminum plates with the BC composite in the middle and applying high voltage to the plates. Forward poling achieved higher output voltage of 170 V and 9.8 μA of current.

4.1.2. Cellulose nanofibrils and cellulose microfibers

Cellulose nanofibrils (CNF) are assemblages of nano-sized (5−60 nm) fibrils (Klemm et al., 2011). Films made from CNF are known for their transparency, flexibility, surface roughness and appliances in green electronics (Fang et al., 2014; Jung et al., 2015; Zhu, Xiao et al., 2013), including the development of TENGs. Yao, Hernandez, Yu, Cai, & Wang (2016) developed a TENG consisting of CNF (320 μm) and fluorinated ethylene propylene (FEP) assembled in In_2O_3 (ITO)/PET substrates. The device reached open-circuit voltage outputs of 5 V, and short-circuit current of 7 μA. However, by increasing the dimensions of the TENG from 1 to 40 cm^2, output voltage and current reached a maximum of 32.8 V and 35 μA.

Roy, Ko, Maji, Van Hai, and Kim (2020) enhanced a CNF-PVDF-based TENG by grafting garlic-extracted allicin onto the CNF film. Surprisingly, the output voltage and current increased in about 6.5 folds compared to the pure CNF film, while the power density increased from 0.25 to 10.13 μW cm^{-2}. It was demonstrated that allicin may serve as a significant cellulose-based TENGs booster. This is mainly attributed to the exceptional dipolar nature of the sulfoxide group, resulting in increased surface triboelectric potential.

Yang, Yao, Yu, Li, and Wang (2017) created a highly degradable aluminum-doped zinc oxide (AZO)-CNF paper-based TENG with enhanced surfaces by applying a plasma treatment or $TiCl_4$ infiltration, although showing limited voltage and current output compared to other CNF-based TENGs in the literature. A hybrid CNF-phosphorene paper was developed by Cui et al. (2017) and used for assembling a TENG with two gold film electrodes. The TENG showed a relatively low open-circuit voltage of 5.2 V and a current density of 1.8 μA cm^{-2}. However, the device was able to withstand exposure to ambient conditions for six months and slightly degrading its electrical outputs.

A hierarchical nanostructured membrane of cellulose microfibers (CMF), CNF and silver nanofibers was constructed by He et al. (2018). Composite membrane served as both friction part and electrode due to its hierarchical construction. A second FEP-silver electrode layer was constructed for the assembly of the TENG, which outputted a maximum of 21.9 V of open-circuit voltage and 0.17 μA of short-circuit current.

I. Kim, Jeon, Kim, You, & Kim (2018) carried out a similar approach by developing two CNF-silver nanowires papers TENG. The optimized silver nanowire content allowed a maximum open-circuit voltage of 21 V and 2.5 μA short-circuit current. Lastly, an unconventional design for a gear-like TENG (Fig. 3a,b) based on CNF and FEP as the friction parts and copper electrodes was constructed by Zhang, Lin et al. (2019). The CNF triboelectricity was improved by adding PEI, a glutaraldehyde crosslinking agent and silver nanoparticle coating, resulting in increased performance. The silver nanoparticles are observed to be uniformly distributed on the surface morphology (Fig. 3c). The TENG was assembled with a different number of gear-like structures (Fig. 3d) and tested different pressure points (Fig. 3e). By increasing the number of gear-like structures from 1 to 3, the open-circuit voltage drastically increased from 122 to 286.5 V (Fig. 3f). However, applying pressure at different angles decreased the overall output voltage to ~27 V (Fig. 3g). Also, the performance of the gear-like TENG was compared to traditional TENG with a planar structure constructed with the same materials (Fig. 3h), proving to be a much more efficient alternative.

4.1.3. Micro- and nanocrystalline cellulose

Microcrystalline cellulose (MCC) is mostly used as a reinforcing agent with excellent properties, like large specific surface area, thermal and mechanical improvement and biodegradability (Trache et al., 2016). Advances in TENG development opted for using MCC or nanocrystalline cellulose (NCC) as the main component. Chandrasekhar, Alluri, Saravanakumar, Selvarajan, and Kim (2017) evaluated the performance of an MCC/PDMS-based TENG. The MCC/PDMS layer was prepared by casting the polymers together. The device worked on vertical contact-separation mode but having the MCC/PDMS film as the only dielectric layer, assembled with two aluminum film electrodes.

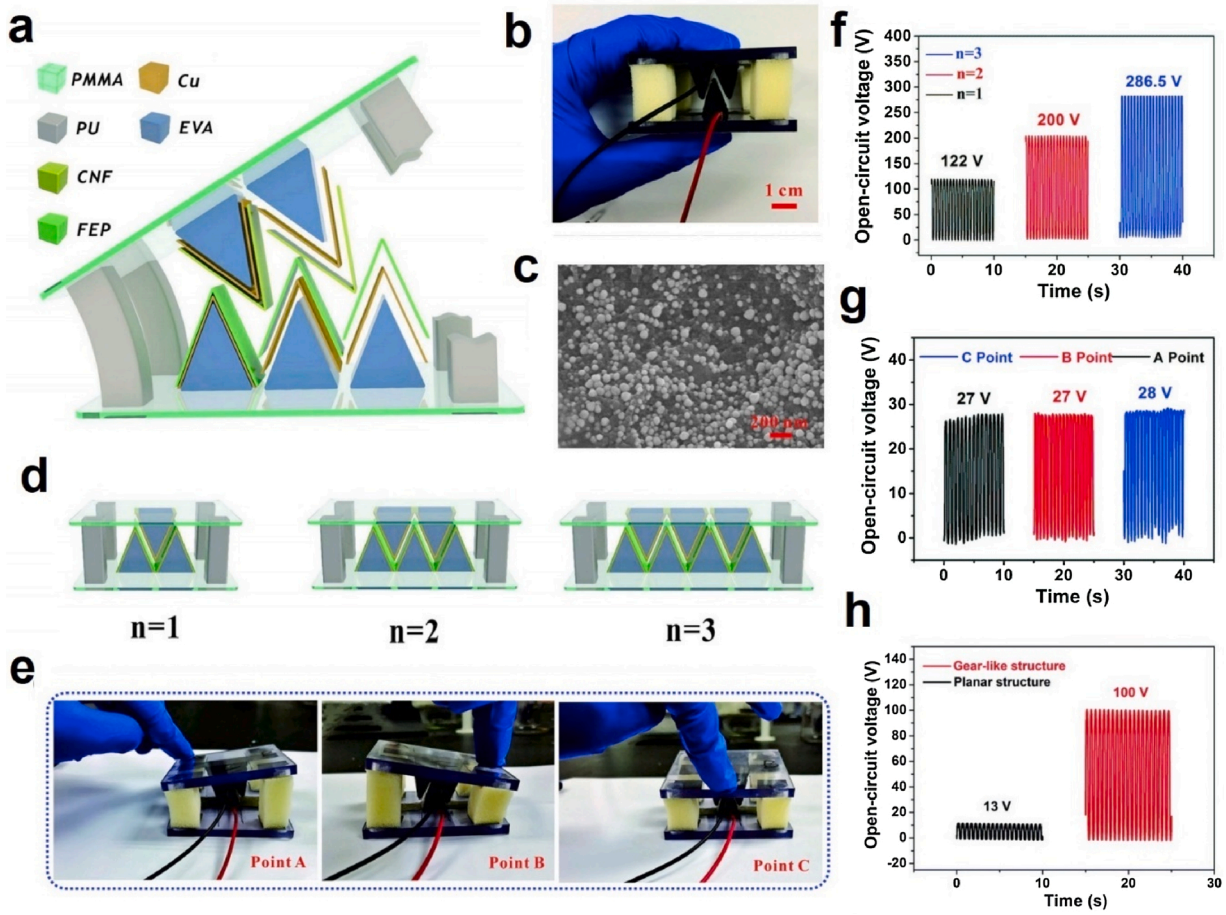

Fig. 3. Schematic illustration of the gear-like TENG and electrical performances. a) Structure of the gear-like TENG, b) Photograph of the gear-like TENG, c) SEM image of the CNF-PEI-silver nanoparticle coating, d) Schematic of the TENG with different number of gear-like structures, e) Photograph of different pressure points, f) Open-circuit voltage at different number of gear-like structures, g) Open-circuit voltage at different pressure points, h) Open-circuit voltage of the gear-like and planar TENG. Reprinted from (Zhang, Lin et al., 2019). Copyright (2019) with permission from Elsevier.

When prepared with 5 % wt MCC, the 3 × 3 cm^2 TENG showed electrical outputs of 28 V and 2.8 μA. Under a similar structure, Peng et al. (2017) opted for coating a PDMS film with NCC flakes. The NCC-coated PDMS layer was set up with two aluminum electrodes for the 1.5 × 1.5 cm^2 TENG assembly. Much higher output was reached, with a peak open-circuit voltage of 320 V and short-circuit current density of 5 μA cm^{-2}. Uddin and Chung (2017) designed a corrugated-core sandwich TENG that permitted both vertical and lateral-sliding contact after being subject to a mechanical force. The core consisted of PET with two subsequent outer layers of aluminum and PI and was fixed between two MCC/aluminum plates. This novel working mechanism exhibited high electrical output performance and allowed for a more efficient multi-corrugated core TENG stack.

4.1.4. Ethyl cellulose

Wang et al. (2017) investigated the performance of ethyl cellulose-(EC) based TENG and a flexible grade 317 L stainless steel (SS) film. The device consisted of the arc-shaped 317 L SS film (50 μm in thickness) as the top layer and EC film (37 μm in thickness) coated to a silver plate as the bottom plate, while silver wires were stuck on the surfaces using Kapton tape. The EC surface was designed using inductively coupled plasma (ICP) etching at various etching powers, resulting in increased surface roughness. Similarly, the 317 L SS surface was enhanced using lithography technology at various pattern densities. The optimized performance was achieved with 275 W of etching power, raising to 176 V of open-circuit output voltage and 31.5 μA of short-circuit current. By adjusting the lithography etching at 4 × 10^4 per mm^2, voltage and current output reached up to 245 V and 50 μA respectively. Šutka et al. (2018) compared the electrical performance of porous EC film in contact with polydimethylsiloxane (PDMS), polymethyl methacrylate (PMMA) and ITO. The highly porous EC surface was achieved by a fast immersion precipitation method. EC-PDMS-based TENG output the highest voltage across a 109 Ω load, reaching 45 V. The same TENG was fabricated with a smooth surface EC, resulting in a voltage reduction to 16 V across the same load. These results agree with electric performance reported by Wang et al. (2017), proving that altering the morphology of the dielectric contact surface could increase the generation of triboelectric charges.

4.1.5. Cellulose acetate

Cellulose acetate (CA) has been used to prepare highly porous, surface-rough films with interesting electronic applications (Meng et al., 2020; Wang et al., 2020). Two studies introduced CA as the main component of TENGs. Srither, Shankar Rao, and Krishna Prasad (2018) compared various positively charged materials for a vertical contact-separation TENG. The results indicated that the pristine cellulose acetate layer had the lowest performances when compared to Kapton, polyurethane and art paper. These results were associated with the combined surface roughness of the materials, rather than the permittivity. Thus, elucidating the need for surface engineering on cellulose layers, as conducted in other studies (e.g., Šutka et al., 2018; Wang et al., 2017). Bai et al. (2020) constructed a TENG exhibiting remarkable electrical output based on a CA/PEI composite paired with low-temperature vulcanized silicone rubber (LTV) and using

commercial conducting fabric as electrodes due to its flexibility and lightweight. The 3 × 3 cm^2 device under optimized CA/PEI mass ratio and thickness delivered up to 478 V, 6.3 μA cm^{-2}, and 2.21 mW cm^{-2} of open-circuit voltage, short-circuit current density and power density respectively. Moreover, the electrical performance remained stable after one month in ambient conditions or 10,800 cycles, proving to be highly durable and reliable.

4.1.6. Nitrocellulose and cellulose paper

Chen et al. (2019) assembled an all-cellulose paper TENG consisting of crepe cellulose papers and nitrocellulose membrane as friction parts and copper foil electrodes in a commercial print paper substrate. The device delivered up to 196.8 V and 31.5 μA even after 10,000 cycles, proving its high performance and durability. Shi, Huang et al. (2019), 2019b) fabricated polypyrrole (PPy)-coated cellulose papers to be used as electrodes in an all-cellulose paper TENG. The single inner friction layer consisted of a nitrocellulose membrane sandwiched between the arc-shaped PPy-coated cellulose papers. The output voltage was lower than the one reported by Chen et al. (2019) but with similar stability and durability after many cycles. Parandeh, Kharaziha, and Karimzadeh (2019) built a TENG based cellulose paper and a polycaprolactone (PCL)/graphene oxide (GO) composite. The high performance of the TENG, reaching up to 120 V open-circuit voltage, 2.5 mA m^{-2} current density and 72.5 mW m^{-2} power density, was attributed to the fibrous surface nanostructured of the materials.

4.1.7. Wood

Wood-based TENGs have been designed as smart-floor and -surfaces appliances (He et al., 2017). Hao, Jiao, Chen, Wang, and Cao (2020) designed an 8 × 8 cm^2 wood-based TENG consisting of New Zealand pine wood and PTFE as the top and bottom layers and a single copper electrode connected to ground. The pressure plate-like TENG reached mean output voltage of 220 V and 5.8 μA. Luo et al. (2019) developed a wood-based TENG under a similar approach. In this case, Balsa wood underwent a chemical process for the fabrication of a fully flexible wood layer. Then, it was fixed to a copper electrode connected to ground and a PFTE layer served as the top layer. The 3 × 3 cm^2 TENG was tested and proposed for the fabrication of a smart ping-pong table with sensing functions that locate the points hit by the ball. The working mechanism of the proposed smart ping-pong table will be further explained in Section 5.4.

4.1.8. Aerogels

Aerogels present unique properties, such as non-fluid colloidal interconnected porous networks, ultra-low density and high specific surface area (Alwin & Sahaya Shajan, 2020; Du, Zhou, Zhang, & Shen, 2013), giving raise to its introduction to novel TENG development. Several studies investigated the suitability and performance of cellulose aerogels as the main component of TENGs. Mi et al. (2018) fabricated a flexible TENG based on a highly porous CNF/polyethylenimine (PEI) aerogel and PVDF nanofiber mat layer (Fig. 4a). The 15–110 nm PVDF nanofibers (Fig. 4b) and CNF nanofibrils (Fig. 4c) deemed for highly porous surface morphology. The vertical contact-separation mode TENG (Fig. 4d) was optimized by adding 10 % wt PEI to the CNF and folding 4 layers of PVDF nanofiber mat, raising to 106.2 V and 9.2 μA of open-circuit voltage and short-circuit current, corresponding to 4.88 W m^{-2} of power density. This represents a power density improvement of 97.6 times the original CNF aerogel and single layer PVDF TENG.

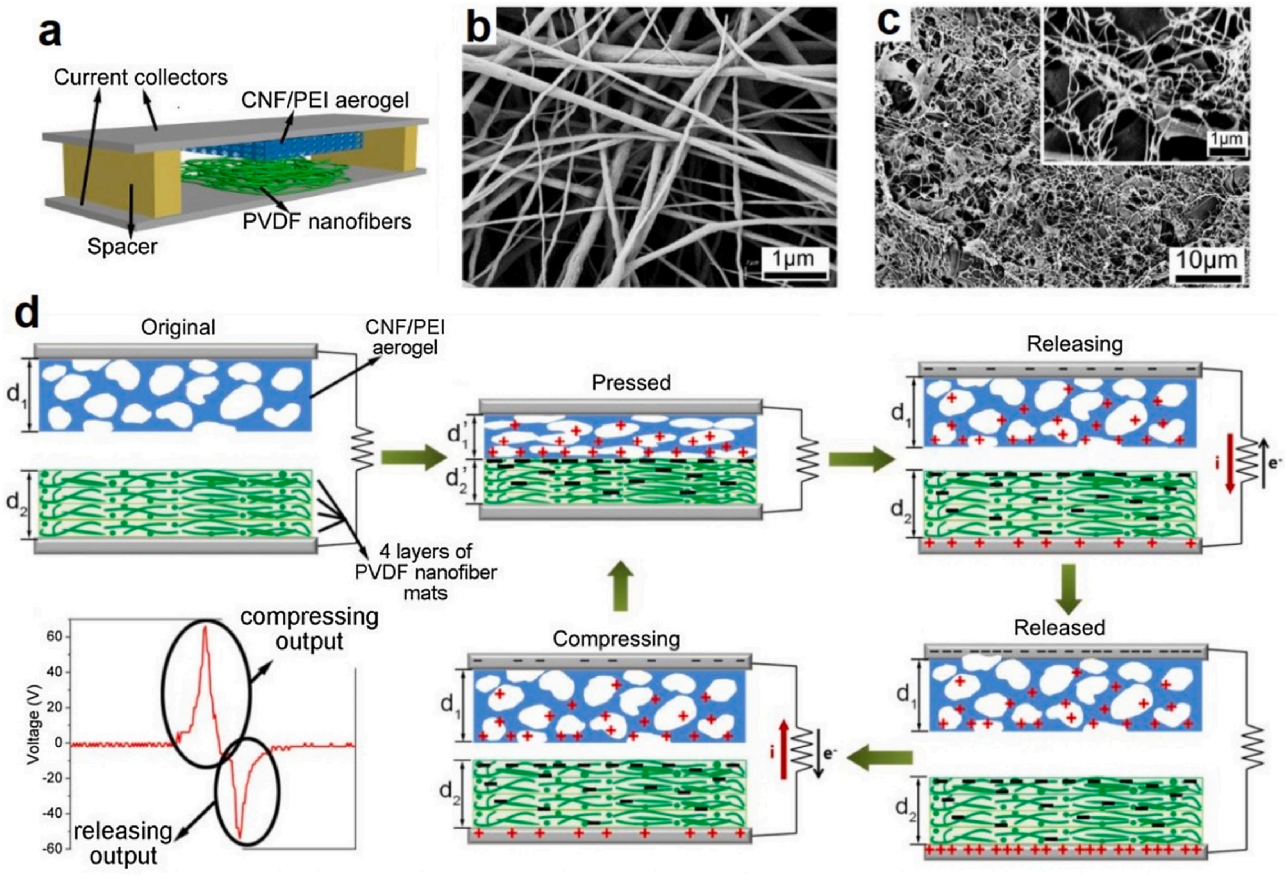

Fig. 4. Schematic illustration of the CNF/PEI TENG, working mechanism and surface morphology. a) Schematic structure of the TENG, b) SEM image of the PVDF nanofiber mat, c) SEM image of the CNF aerogel, d) operating principle of the TENG. Reprinted from (Mi et al., 2018). Copyright (2018) with permission from Elsevier.

A similar approach was investigated by Beyranvand and Gholizadeh (2020) with a multi-layer PDMS, carboxymethyl cellulose (CMC)/PVDF or PDMS aerogel, PVDF, Kapton and aluminum foil electrodes in various arrangements. The PDMS/CMC-PDMS aerogel/PDMS/Kapton arrangement resulted in the highest open-circuit voltage of ~14 V and ~0.22 μA of short-circuit current. Shi, Huang et al. (2019) developed a hybrid PENG-TENG based on cellulose-$BaTiO_3$ aerogel with aluminum electrode. The single PENG delivered up to 15.5 V and 3.3 μA of output voltage and current. By coupling a single-electrode TENG to the PENG, the maximum output voltage reached 48 V. Zhang et al. (2020) fabricated a conventional cellulose II aerogel-PTFE film-based TENG with aluminum foil electrodes. An open-circuit output of ~65 V was observed at different frequencies and 1.86 μA at 4 Hz. The cellulose II aerogel TENG performance was further enhanced by adding other polysaccharides, namely chitosan and alginic acid, to the aerogel. Qian et al. (2019) introduced an all-printed 3D micro/nano hierarchically patterned structure for a CNF aerogel-PDMS TENG. The silver electrodes, CNF aerogel and PDMS layers were printed directly on PET substrates and assembled in a vertical contact-separation structure. The friction layers were printed in three different arrangements in order to obtain three different contact angles ($\theta = 90°$, 45° and 0°). Results showed that the printed contact angle influenced the electric performance, being $\theta = 0°$ the best performance arrangement. It is suggested that the contact angle impacts over the effective contact area between tribo-layers.

4.2. Chitosan

Chitin is a natural biopolymer extracted from crustacean exoskeleton (Pandey, Singh, Momin, & Bhavsar, 2017). Chitosan is obtained after the deacetylation of chitin. The deacetylated β-(1,4)-linked D-glucosamine units may serve as an electron-donating group (Zhang et al., 2020). Some studies explored various chitosan nanocomposite films as potential triboelectric layers in vertical contact-separation TENGs with enhanced properties and performance. Jao et al. (2018) developed a chitosan-based TENG consisting of a prepared chitosan-glycerol film with a nanostructure surface and a PTFE layer using aluminum sheets as electrodes. The optimized TENG allowed for an output voltage of 130 V with the contact area of 5×3 cm^2. Wang et al. (2018) prepared multiple nanocomposite films based on chitosan and starch, lignin, glycerol or acetic acid. The nanocomposite films displayed different characteristics in terms of surface morphology, stretchability, triboelectric potential and degradability. The TENG layers consisted of the nanocomposite and Kapton films attached to copper electrodes. The chitosan nanocomposite with 10 % acetic acid achieved the best voltage and current performance due to the electron-donating nature of acetic acid. This agrees with the results of Yu et al. (2020), in which chitosan, along with lignin, are regarded as the ideal positively charged biomaterials for TENG applications. Lastly, an unconventional chitosan-diatom TENG was developed by Kim, Lee, Kim et al. (2020). The purpose of this nanocomposite is to improve the performance of the chitosan TENG with diatom frustule due to its nanoporous structure and high surface area. By embedding 0.1 % diatom frustule, the 3×4 cm^2 TENG reached up to 150 V of output performance and enhanced the average power density in 3.7 times. As evidenced in the studies summarized in this section, chitosan is considered as one of the preferred positively charged biomaterials and known to be able to further improve their triboelectric characteristics under several treatments and synergic additives for conventional TENG applications. Regarding chitin, Jiang et al. (2018) assembled bio-TENGs with several biomaterials (i.e. chitin, cellulose, egg white, silk fibroin, and rice paper) in many arrangements. The chitin-egg white and chitin-rice paper TENGs delivered the lowest electrical performances in terms of output voltage and current. This is attributed to the rank of chitin in the triboelectric series, which is not far enough from the materials with the highest (egg white) and lowest (rice paper) transferred charges. Hence, pure chitin is not suitable for the development of highly efficient TENGs. To improve the performance of chitin-based TENGs, materials engineering techniques are required.

Chitosan has also been used for the preparation of hydro- and aerogels. Composite hydrogels were developed by Wang and Daoud (2019), involving chitosan hydrogel with embedded silver nanowires and crosslinked by silver or copper ions that served as the electrode. The hydrogel was sandwiched between PDMS layers as a single-electrode TENG for human motion harvesting. The model proved to be washable, allowing to regain the loss of performance due to dehydration. Zheng et al. (2018) prepared chitosan- and CNF-based aerogels for positively charged layers and PI aerogels or PDMS sponge as negatively charged layers in various assembles. As a reference, the same setup was carried out by assembling dense film CNF, chitosan, and PDMS. Interestingly, the aerogel CNF/PDMS and chitosan/PDMS assemblages enhanced power density 8 and 11 times compared to the dense film assemblages. Porous chitosan/PDMS aerogels showed the highest electric performance, outputting 30 V of voltage and 3.4 μA of current. Additionally, a cellulose II aerogel-based TENG (Zhang et al., 2020) was further improved by adding chitosan with 82.4 % degree of deacetylation. The highest cellulose-to-chitosan mass ratio (2:1) resulted in the best performance. The open-circuit output voltages increased with the cellulose-chitosan aerogel diameter, being 242 V the highest at 35 mm in diameter. Interestingly, increasing the aerogel thickness resulted in improved output performance, which contradicts other studies with dense biopolymer films (e.g., Ccorahua, Cordero, Luyo, Quintana, & Vela, 2019, 2019b; Pang et al., 2018). The opposing behavior between dense and highly porous materials may be attributed to the generation of triboelectric charges in the surfaces of inner pores due to electrostatic induction (Jang et al., 2016; Lee et al., 2014). Hence, thicker aerogels may induce more triboelectric chargers under the increasing surface area.

4.3. Starch

Ccorahua, Cordero et al. (2019) fabricated a starch-cellulose-based TENG by extracting starch from Andean white potato (*Solanum tuberosum*) (Fig. 5a) and turned into starch films using sandpaper as a substrate for microstructured surface morphology (Fig. 5b) ranging from about 50–200 μm in thickness (dielectric 1). The starch films were coupled to mixed cellulose ester films (dielectric 2) and covered in aluminum foil as the electrodes. The 4 cm^2 TENG electric output reached up to 300 mV when coupled to the thinnest starch film, although the thicker films lowered the output to about 60 mV. Further research by Ccorahua, Huaroto et al. (2019) characterized both flat and microstructured starch film (Fig. 5c,d) and created a third starch electrolyte film by adding $CaCl_2$ salt and casting the microstructured film under the same conditions. The dielectric films and aluminum electrodes were stuck together using double-sided tape. The working model can be observed in Fig. 5e and a photograph of the starch layer in Fig. 5f. Similar to their previous results, the electrical output increased with decreasing starch film thickness, reaching up to 300 mV for a 35 μm thick film (Fig. 5g). Moreover, the output increased with higher applied loads (3, 4, 6, 8 and 10 N) and higher frequencies until reaching 4 Hz. It was observed that frequencies higher than 4 Hz did not make a significant improvement in the electrical output. Regarding the electrolyte starch-based TENGs, the 0.5 % wt/wt $CaCl_2$ starch films showed the highest voltage output and current density, scaling up to three times the voltage and current output presented by the starch-only TENG. This is due to the cation/anion balance between the two dielectric layers influencing over the triboelectric effect when coming into contact. In the case of $CaCl_2$, it has been demonstrated that when added to the dielectric polymer, it can turn it into a more positive triboelectric material (Ryu et al., 2017). Hence, an asymmetric pairing of cations and anions can be reduced by adding salt at the right concentration (polymer electrolytes) and reaching higher electrical outputs.

A high-output corn starch-based TENG was developed by Sarkar,

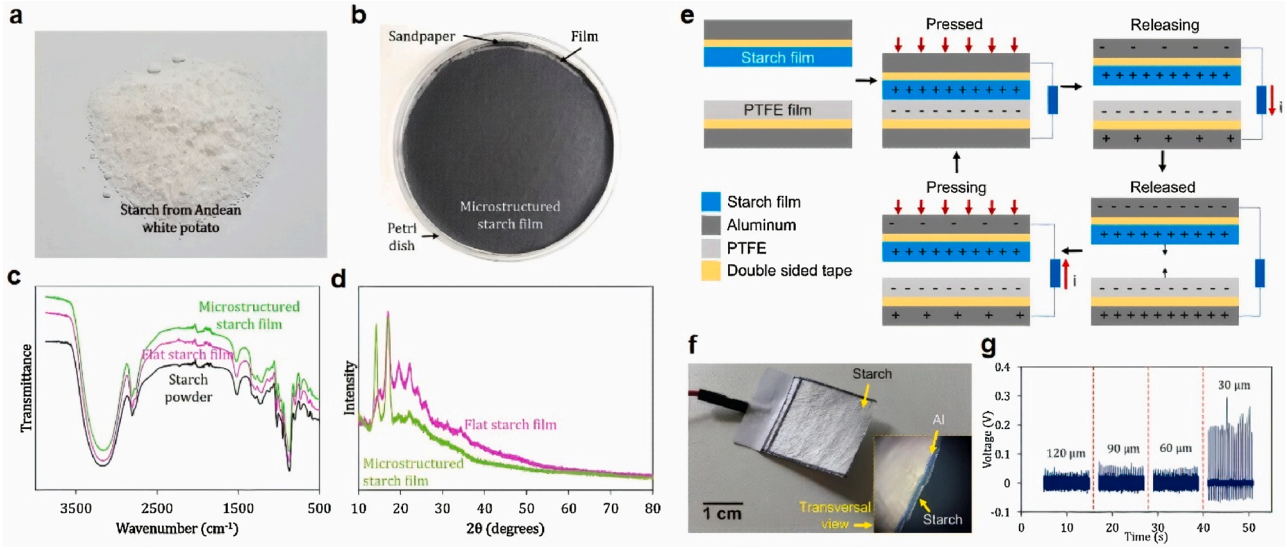

Fig. 5. a) Andean white potato starch; b) microstructured potato starch film on sand paper; c) ATR-FTIR spectra of the starch powder, flat starch film and microstructured starch film; d) crystallinity of the flat and microstructured starch films; e) working mechanism of the starch-PTFE TENG in vertical contact-separation; f) Photograph of the starch film layer covered by aluminum foil; g) electric output as a function of starch film thickness. Reprinted from (Ccorahua, Huaroto et al., 2019). Copyright (2019) with permission from Elsevier.

Kamilya, and Acharya (2019). This TENG consisted of a 0.15 mm thick corn starch and 0.20 mm PDMS films as dielectric layers coupled to carbon tapes as electrodes in a vertical contact-separation mode. The 15 cm^2 TENG was mounted to an arch-shaped PET substrate allowing to release after applying a mechanical stimulus. The open-circuit output voltage raised to ~560 V at 0.18 mA. This TENG was able to power over 100 commercial blue LEDs directly and is tested for mechanical energy harvesting during human walking.

Contrary to the previous starch-based research, Zhu, Xia, Xu, Lou, and Zhang (2018) built a wearable single-electrode TENG for human perspiration sensing. The assemble is simple, consisting of starch paper (~1 mm thick) with a metallic electrode connected to a load. Upon water spraying, a water network is created and the starch paper's resistance is reduced from 19 MΩ to 130 KΩ after several sprayings. The output voltage across the load increases with every spray, reaching and stabilizing at ~14 V after the 5^{th} spray. Similar behavior was observed after testing the device attached to a human elbow and experiencing repeated flexion and extension motion, measuring higher voltage outputs under longer motion time. It is suggested that presented TENG may serve for human perspiration and motion sensing. However, the durability of the device may pose a major frontier to reach this endpoint.

4.4. Alginate

A soluble and recyclable TENG based on sodium alginate (SA) and PVA as dielectrics and lithium and aluminum electrodes was developed by Liang et al. (2017) (Fig. 6a). The SA film characterizes for being transparent, flexible and thin (500 nm) (Fig. 6b,c). The dissolution process consists of PVA and SA films and lithium electrode dissolving upon contact with water. The hydrogen gas created by the lithium + water reaction facilitates the dissolution, while the resulting LiOH reacts with the aluminum electrode, decomposing it (Fig. 6d). A complete dissolution is observed after 10 min immersed in water. By working in vertical contact-separation mode (Fig. 6e), the SA-based TENG outputs 1.47 V and 3.9 nA under finger motion (Fig. 6f,g). The output voltage increases with amplitude (Fig. 6h,i), and a similar trend is observed with respect to frequency (Fig. 6j,k). The presented SA-based TENG displays an interesting breakthrough on eco-friendly devices, as it completely disappears in an aqueous solution without leaching hazardous chemicals or materials. Further development must focus on improving the energy-harvesting efficiency.

Pang et al. (2018) opted for calcium alginate- (CA) based TENG by adding a 5 % (w/w) $CaCl_2$ solution to the fabricated SA film. SEM images revealed rough porous structures on the CA film surface, which is beneficial for triboelectric power generation. The working model involved the CA film as the sole dielectric layer (thickness ranging from 50 to 350 μm) and a top and bottom surfaces aluminum electrodes. The electrical characteristics of the CA-based TENG showed open-circuit voltage and short-circuit current raising to 38 V and 245 nA respectively. Such output was achieved by using the thinnest CA film, while thicker films reduced the electrical performance. Degradation tests indicated a CA film (100 μm) weight loss of almost 100 % after 72 h immersed in saline water (resembling seawater).

The performance of the cellulose II aerogel-based TENG previously described was also tested by introducing alginic acid. The carboxylic acid group present in the β-D-mannuronate and α-L-guluronate units allows for electron withdrawal in the cellulose-alginic acid composite aerogel. However, alginic acid content higher than 0.5 % considerable reduced the output voltage when compared to the reference (pristine cellulose II aerogel). This trend is due to the electron-withdrawal groups in alginic acid against the second dielectric layer (PTFE), a tribo-negative material. These results oppose to the cellulose-chitosan composite aerogel TENG aforementioned (Zhang et al., 2020), mainly attributed to the electron-donating groups present in chitosan.

Jing et al. (2020) synthesized a transparent and elastic PVA-SA hydrogel for TENG applications. The hydrogel consisted of 8 % wt PVA and SA ranging from 1 to 4 % wt. A borax solution (8 % wt) was mixed with the hydrogel and then immersed in a $CaCl_2$ solution (1 mol L^{-1}). The resulting hydrogel encompassed borax crosslinked PVA networks and calcium crosslinked alginate networks as described by Li et al. (2018) and Han, Lei, and Wu (2014). Moreover, Na^+, Ca^+, Cl^- ions were present from the CaCl2-alginate exchange and $B(OH)_4^-$ ions from borax. The supermolecular networks allowed for improved self-healing property and elasticity, while the ions enhanced the conductivity of the hydrogel. A single-electrode TENG was assembled by filling a PDMS bag (1 mm interior thickness) with the hydrogel attached to an aluminum current lead connected to ground and using aluminum as the tribo-positive counterpart. The highest output voltage (96.6 V) and current (7.2 μA) was achieved by the 2 % SA hydrogel. By connecting the current lead to the aluminum layer, the now double-electrode model

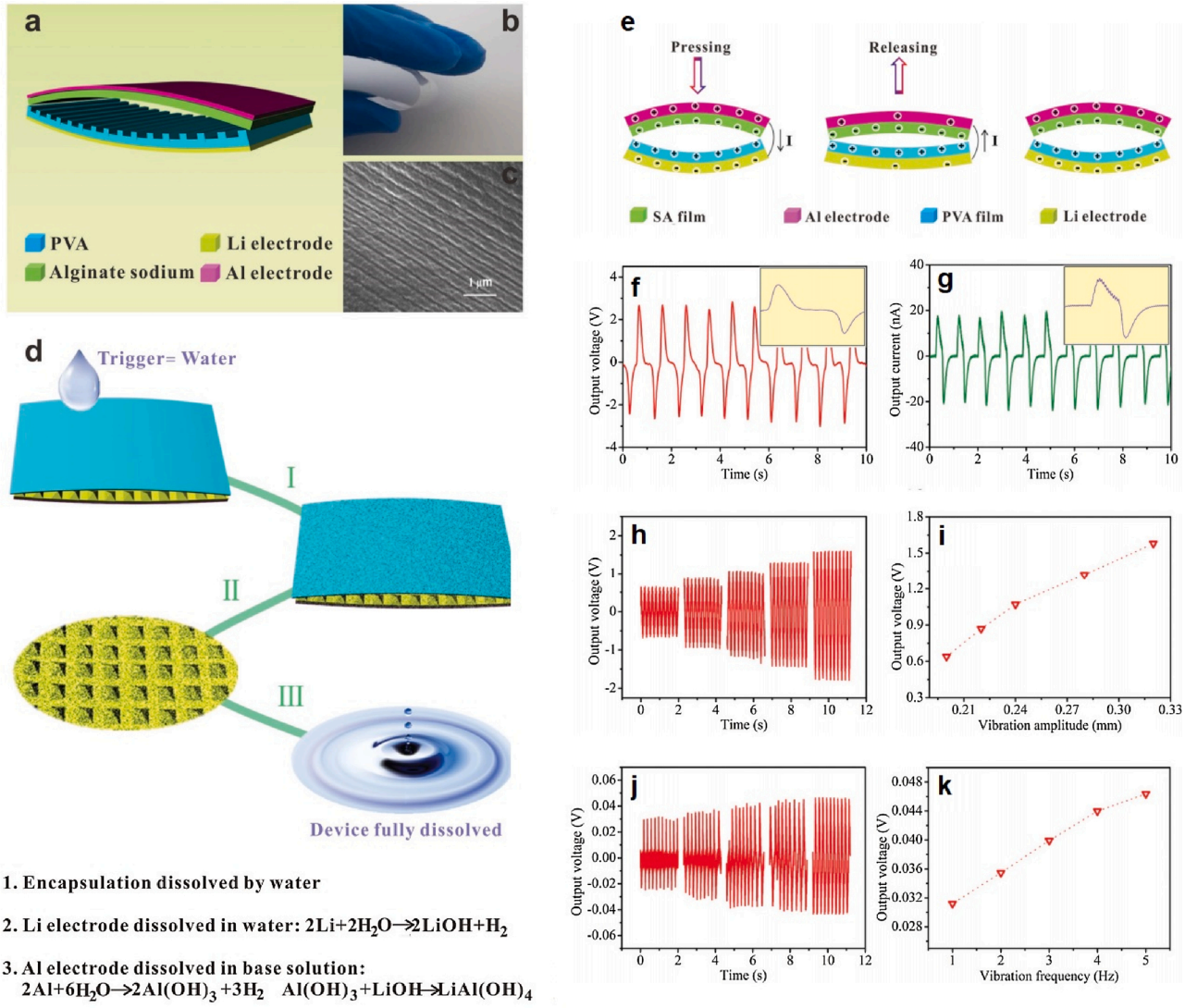

Fig. 6. SA-based TENG schematics and outputs. a) Schematic of the SA-based TENG; b) Photograph of the SA film; c) SEM image of the SA film; d) dissolution process and chemical reactions involved; e) working mechanism of the SA-based TENG; f) regular voltage output; g) regular current output; h) output voltage as a function of vibration amplitude; i) summarized output voltage v. vibration amplitude; j) output voltage as a function of vibration frequency; k) summarized output voltage v. vibration frequency. Reprinted from (Liang et al., 2017). Copyright (2017) with permission from Wiley-VCH.

output up to 203.4 V and 17.6 μA. The significant improvement in the output performance by the double-electrode model is due to the increased electrostatic potential difference between PDMS and aluminum when compared to PDMS and ground. Hence, the double-electrode mode is regarded as optimum.

4.5. Pullulan

Lu, Li, Ping, He, & Wu (2020) investigated the performance and recyclability of a pullulan-based TENG, including various additives: glycerol, NaF, trehalose, bovine serum albumin (BSA) and carboxymethyl cellulose (CMC). A pullulan-pure and five pullulan-based films (64 cm^2) were prepared by mixing 7.5 ml (10 % wt) pullulan solution with 7.5 ml BSA, CMC, glycerol at 1 % wt or 0.1 M in the case of NaF and trehalose. Kapton film was used as the second dielectric and silver and aluminum foils as electrodes in a vertical contact-separation mode (Fig. 7a). All of the additives enhanced the electrical output compared to the pullulan-pure film (Fig. 7b). Fig. 7c,d display the voltage output of the six films at 10 Hz and 10 W respectively, and Fig. 7e the output power with loading resistance ranging from 100 Ω to 1 G Ω. The highest open-circuit voltage achieved was 79 V by the NaF-pullulan-based TENG, and the lowest by the pullulan pure film (46 V). Importantly, recycling tests were carried out (Fig. 7f) to evaluate the performance of pullulan films after reused. It was evidenced that even after five reassembles, the pullulan film remained consistent with respect to open-circuit output at various loading powers (Fig. 7g,h). Thus, proving to be high-performance and high recycling potential material for TENG applications. To the best of our knowledge, this is the only publication investigating pullulan-based TENGs.

5. Potential applications

In the recent progress of polysaccharide-based TENGs, multiple approaches and working modes have been carried out. Most researchers concentrated on the traditional vertical contact-separation mode using cellulose derivatives, although the electrical performance varied greatly among studies. It has been discussed that the chemical composition of each polysaccharide influences over the triboelectric charges they possess, thus affecting the suitability to be assembled with certain materials due to similar or opposing chargers. For instance, the β-(1,4)-linked D-glucosamine units in chitosan serve as strong electron-donating units due to its amine groups. In contrast, the β-D-mannuronate and α-L-

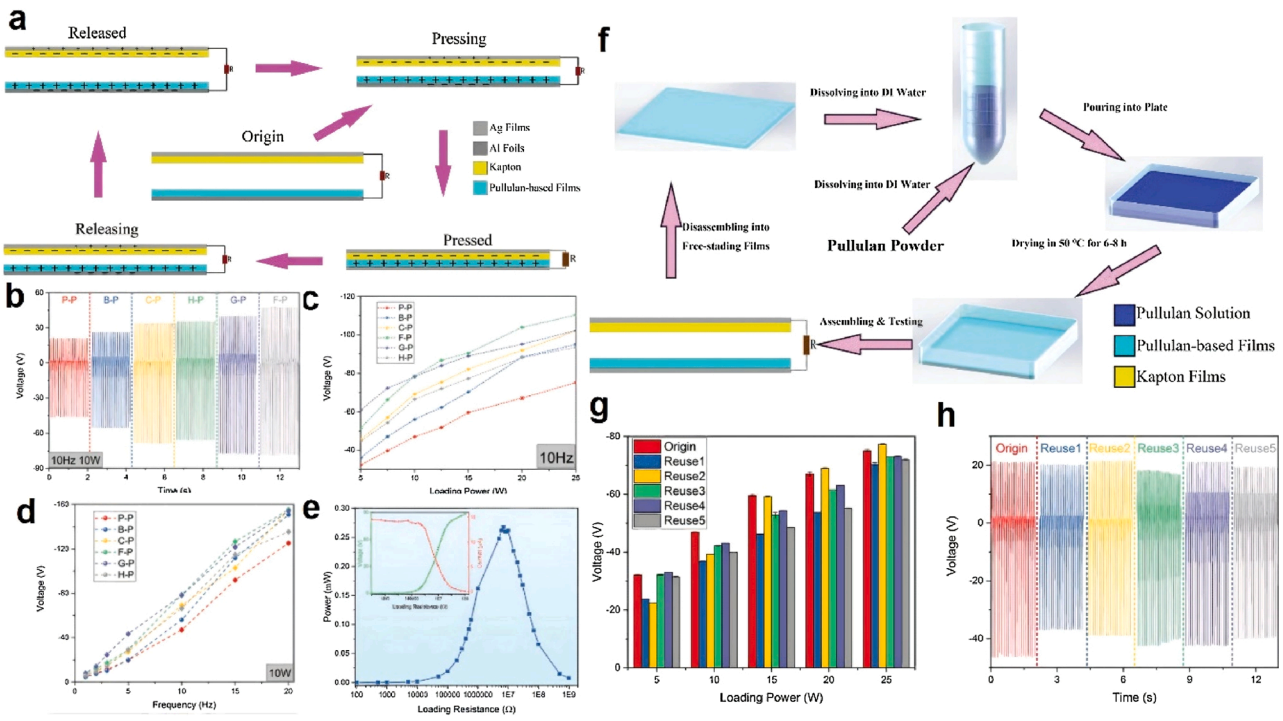

Fig. 7. Working schematic, performance and degradability of the pullulan-based TENGs. a) vertical contact-separation mode scheme; b) open-circuit output voltages; c) summary of the voltage output at 10 Hz; d) summary of the voltage output at 10 W of loading power; e) output power at various loading resistances; f) recycling mechanisms of the pullulan film; g) summary of the open-circuit output voltage after various reuses; h) open-circuit voltage curves after various reuses. Reprinted from (Lu et al., 2020). Copyright (2020) with permission from Wiley-VCH.

guluronate units in alginate have electron-withdrawing carboxylic acid groups. Regarding other polysaccharides, namely cellulose consists of β(1,4)-linked D-glucose units, pullulan consists of α-(1,6) and α-(1,4)-linked maltotriose units, and starch of mainly amylose (α-(1,4)-linked D-glucose units) and amylopectin (α-(1,4)-linked D-glucose units and α-(1–6)-branch linkages). Indeed, the right choice of materials is crucial to increase the electrical performance of TENGs (Zhang et al., 2020). However, many of the physical and chemical treatments described in the previous section play an important role in the overall performance of polysaccharide-based TENGs.

Apart from experimental TENG assemblages and measurements, a whole spectrum of TENG practical application has been reported in the literature. Ranging from water, wind, biomechanical energy harvesting, to wearable self-powered active sensors for medical and health monitoring applications, TENGs are proven to be extremely versatile. In this section, we reviewed the progress in realistic applications of conventional TENGs and discuss the potential and practical applications of polysaccharide-based TENGs reported in the literature.

5.1. *Environmental energy harvesting*

Remarkable progress has been made regarding ocean wave, raindrop, ultrasonic and wind energy harvesting utilizing TENG technology. These energy sources are renewable and address the environmental issues caused by fossil fuel consumption. Air-flow energy scavenging can be achieved by elasto-aerodynamics-driven TENG working on the same principle as vertical contact-separation mode (Wang, Mu et al., 2015). The main components of this design, Kapton and PTFE, can be partially replaced by biopolymer alternatives with similar triboelectric charges and extended durability and reliability (Bai et al., 2020). For instance, Srither et al. (2018) designed a flexible CA and PTFE based TENG that could potentially replace commercial Kapton. Also, Oh et al. (2019) assembled a BC and PTFE TENG with high electrical performance (i.e. 170 V of open-circuit voltage). By partially replacing synthetic materials, the grade of degradability of the device increases, making it easier for recycling and processing at the end-of-life. Another design of an undulating film for bidirectional wind energy harvesting included Kapton as the main component (Quan, Han, Jiang, & Wang, 2016). The practical viability of replacing the positively charged layer with polysaccharide-based materials with similar triboelectric charge density required further research.

Ocean wave and tidal energy harvesting is a major challenge. Most generators are known for being difficult to manufacture, expensive and bulky (Tian et al., 2020). Under this context, emerging TENG technology is a promising alternative for highly efficient and cost-effective water wave energy harvesting. The proposed designs encompass large-scale networks of enclosed and freestanding TENG with a rolling ball inside the enclosure (Wang, Niu et al., 2015) or wave-driven polymer-metal electrode contact hit by a moving ball in floating setups (Chen et al., 2015). Regarding polysaccharide-based TENGs, Pang et al. (2018) designed a PLA case for enclosing their CA-based TENG. The case was tested for wave energy harvesting in a pool with a set of four springs holding the top layer of the TENG, showing great potential in blue energy harvesting.

5.2. *Biomechanical energy harvesting and motion sensing*

Biomechanical energy refers to the many forms of daily human motion, like walking, arm and hand stretching, breathing, etc., that represent a source of mechanical energy that is wasted. Given the increasing development in wearable and biocompatible TENGs, some ways of harvesting biomechanical energy have been proposed. One of the first ways to harvest biomechanical energy that was explored was through walking. In this case, the first synthetic-based TENGs were mostly inserted in common shoes and are activated by the press and release motion while walking (Hou et al., 2013; Huang et al., 2014). Wearable and stretchable fabrics that induce triboelectric energy are another common approach to human motion harvesting (Kim et al.,

2015; Zhou et al., 2014).

For this particular application different polysaccharide-based TENGs have been developed. Many of the polysaccharide-based TENGs presented in Section 4 tested the viability of their designs for human motion and movement sensing and energy harvesting. The CNF aerogel-based TENG fabricated by Qian et al. (2019) was also used as a human self-powered motion sensor. The device was attached to the hands and legs of a person walking, proving to be a viable alternative for providing bio-feedbacks and physiological evaluation. Kim et al. (2018) developed a CNF/AgNWs e-paper TENG. Writing and erasing tests on the e-paper TENG using a pencil and eraser delivered electrical outputs dependent on the pressure applied for any of these actions. The re-writability of the e-paper elucidates its potential application for external input sensing. Kim, Lee, Kim et al. (2020) used the chitosan-diatom TENG for motion sensing while attached on wrist, elbow, knee and ankle, driven by a wide range of joint movements. Bai et al. (2020) sewed their CA/PEI-based TENG to the inner part of a pocket for wearable self-powered sensing. This pocket showed a response to multiple mechanical stimuli, potentially serving in the field of human-machine interaction. Shao et al. (2019) integrated their BC TENG to a rehabilitation device based on hand motion and onto regular clothing. Their approach allowed for harvesting small mechanical energy from human motion. TENG-integrated shoes for locomotion energy harvesting is fairly common. An interesting self-powered charging unit was designed by Chandrasekhar et al. (2017). The design integrated a full bridge rectifier, capacitors and a Li-ion battery to the MCC-based TENG, that worked as the power source.

5.3. Biomedical and healthcare monitoring

The potential applications of TENGs in the medical field are very diverse. Synthetic polymer-based TENGs have been designed for cardiac pacemakers powered by animal breathing (Zheng et al., 2014), electrical stimulation for cell modulation (Tian et al., 2019), nerve stimulation (Lee et al., 2017), implantable drug delivery system (Song et al., 2017), healthcare monitoring (Bai et al., 2014; Zhao, Yan et al., 2016) among many other appliances. Although TENG technology for biomedical applications has come a long way, not much has been reported for polysaccharide-based TENGs. The CMF/CNF/Ag-based TENG by He et al. (2018) served for breathing monitoring, $PM_{2.5}$ removal and excellent antimicrobial activity. To the best of our knowledge, this is the only study to test the potential healthcare monitoring application of a polysaccharide-based TENG. Other studies suggested EC-based (Wang et al., 2017) and sodium alginate-based TENGs (Liang et al., 2017) as promising alternatives for power solution in biomedical implants, but without conducting the procedure *in vivo*.

Ideally, body implantable devices for healthcare monitoring should be biodegradable and not include materials that may release toxic chemicals (Maiti et al., 2019). By including polysaccharides as the main component of biomedical TENGs, the amount synthetic polymers with potentially toxic chemicals, like flame retardants or endocrine disrupting substances (Lithner, Larsson, & Dave, 2011), are considerably reduced.

The biodegradability nature of polysaccharides can be exploited to design novel TENGs that serve as power source for implantable or ingestible health care electronics for continuous monitoring or diagnosis and treatment of the human body. These implantable medical devices (IMD) include sensors, cardiac peacemakers, and defibrillators, among others (Jiang et al., 2018). The batteries these IMDs use need to be removed after their service life is reached. Biocompatible and bioabsorbable TENGs can be produced using polysaccharides as the friction layers in combination with inert metals as electrodes. For instant, Jiang et al. (2018) used cellulose and chitosan as the friction layers of a bioabsorbable TENG. They used rice paper as substrate and a thin magnesium layer as electrode. They were able to adjust the operation time of this TENG from days to weeks using other bioabsorbable materials for encapsulation. The in-vivo tests showed that after completing its function, this TENG was degraded and fully absorbed in rats.

Other studies tested the hydrolytic degradation of polysaccharide-based TENGs (Dong et al., 2017; Yang et al., 2017). In general, complete degradation of the TENGs can be achieved in a short period of time. The main issue with biodegradable TENGs is the rapid loss of performance after hydrolytic degradation starts. To tackle this issue, Zheng et al. (2016) investigated the in vivo biodegradability of bio-TENGs implanted in rats. The short- and long-term degradability of the bio-TENGs were controlled by encapsulating the implanted TENGs in either PVA or poly(L-lactide-co-glycolide) (PLGA). After nine weeks, the implanted bio-TENGs had biodegraded almost completely in the animal body. Several polysaccharides have proved to be suitable for high-performance TENGs with excellent hydrolytic degradation. However, in vivo studies are still lacking.

5.4. Internet of Things (IoT)

The Internet of Things (IoT) is a technological paradigm of paramount networks and interconnected machines and devices (Lee & Lee, 2015). In recent years, the IoT has gained increasing attention from the scientific community and industry. It is no surprise that with the vast practical applications and versatility of TENG devices, they are prone to become one of the major drivers of the IoT. The majority of the "smart things" and devices proposed in the literature are still in the early stages of development. However, these may serve as the first step into a futuristic reality of ubiquitous connections.

Chen et al. (2019) printed a small-scale piano keyboard with nitrocellulose-based TENGs under each tile. The design included bridge rectifiers and capacitors connected to the TENG as the sole source of energy and a laptop through a microcontroller. The microcontroller permitted real-time communication between the keys and the computer, being able to play simple songs. The concept of smart floors was further developed by Hao et al. (2020) with a wood-based TENG. They suggest that smart floors may help track and record the movement of dancers in large-scale applications. Lastly, Luo et al. (2019) proposed a solution for a common mistake in referees' decision in table tennis matches regarding top or side edge balls. By attaching their flexible wood-based TENG on the edge and side of the table, the force of the ball hitting the surface of either will send a signal to determine whether top or side edge ball happens.

6. Conclusions and future perspectives

In recent years, TENG research has made great progress in all possible directions. One of the most recent lines of research is the field of eco-friendly, degradable and waste-free TENGs for sustainable development. In this review, we described the current knowledge regarding polysaccharide-based TENGs, the materials aspects involved in their development and potential applications in various industrial branches. In general terms, polysaccharide-based materials showed promising characteristics for the development of highly efficient and green TENGs. Many of the synthetic polymers commonly used as dielectric layers can be replaced by polysaccharide materials as they exhibit similar triboelectric charge densities. In addition, polysaccharides are biodegradable and highly biocompatible. The procedures for enhancing TENG performance, such as surface engineering and end-functional group change, are viable and have been successfully carried out in polysaccharides. Many studies focused on developing and reporting TENGs based on cellulose and its derivatives, chitosan, alginate, starch and pullulan. The overall electrical performance reported by these studies is highly variable. However, surface roughness, conductivity, and triboelectric enhancement are common ways to achieve the highest performance. Most studies opted for a traditional vertical contact-separation mode and a few for the single-electrode mode.

The most significant benefit of polysaccharide-based TENGs is their

biocompatibility, degradability and negligible environmental impact. In spite of this, the practical appliances are poorly studied, with only a few studies carried out tests for the suggested applications. As biomaterials are recognized for their biocompatibility, the development of bio-TENGs are of special interest for healthcare monitoring. It is necessary that future TENG research leans towards sustainable alternatives in realistic scenarios, including body implantable bio-TENGs, in situ environmental energy harvesting, wearable high-quality electronics and self-powered IoT devices. For this matter, polysaccharides are proposed as a suitable alternative and it is encouraged to continue studying and developing TENGs on this line of research.

Declaration of Competing Interest

The authors report no declarations of interest.

Acknowledgements

This work was supported by the Vice-rectorate of Research of the Pontificia Universidad Catolica del Peru (VRI-PUCP).

References

Alwin, S., & Sahaya Shajan, X. (2020). Aerogels: Promising nanostructured materials for energy conversion and storage applications. *Materials for Renewable and Sustainable Energy, 9*(2), 3. https://doi.org/10.1007/s40243-020-00168-4

An, S., Sankaran, A., & Yarin, A. L. (2018). Natural biopolymer-based triboelectric nanogenerators via fast, facile, scalable solution blowing. *ACS Applied Materials & Interfaces, 10*(43), 37749–37759. https://doi.org/10.1021/acsami.8b15597

Bai, P., Zhu, G., Jing, Q., Yang, J., Chen, J., Su, Y., … Wang, Z. L. (2014). Membrane-based self-powered triboelectric sensors for pressure change detection and its uses in security surveillance and healthcare monitoring. *Advanced Functional Materials, 24*(37), 5807–5813. https://doi.org/10.1002/adfm.201401267

Bai, Z., Xu, Y., Zhang, Z., Zhu, J., Gao, C., Zhang, Y., … Guo, J. (2020). Highly flexible, porous electroactive biocomposite as attractive tribopositive material for advancing high-performance triboelectric nanogenerator. *Nano Energy, 75*, Article 104884. https://doi.org/10.1016/j.nanoen.2020.104884

Beyranvand, M., & Gholizadeh, A. (2020). Facile and low-cost synthesis of flexible nanogenerators based on polymeric and porous aerogel materials. *Current Applied Physics, 20*(1), 226–231. https://doi.org/10.1016/j.cap.2019.11.009

Boisseau, S., Despesse, G., & Ahmed, B. (2012). Electrostatic conversion for vibration energy harvesting. *Small-scale energy harvesting*. https://doi.org/10.5772/51360

Ccorahua, R., Cordero, A., Luyo, C., Quintana, M., & Vela, E. (2019). Starch-cellulose-based triboelectric nanogenerator obtained by a low-cost cleanroom-free processing method. *MRS Advances, 4*(23), 1315–1320. https://doi.org/10.1557/adv.2018.652

Ccorahua, R., Huaroto, J., Luyo, C., Quintana, M., & Vela, E. A. (2019). Enhanced-performance bio-triboelectric nanogenerator based on starch polymer electrolyte obtained by a cleanroom-free processing method. *Nano Energy, 59*, 610–618. https://doi.org/10.1016/j.nanoen.2019.03.018

Chandrasekhar, A., Alluri, N. R., Saravanakumar, B., Selvarajan, S., & Kim, S. J. (2017). A microcrystalline cellulose ingrained polydimethylsiloxane triboelectric nanogenerator as a self-powered locomotion detector. *Journal of Materials Chemistry C, 5*(7), 1810–1815. https://doi.org/10.1039/c6tc05104a

Chang, T. H., Peng, Y. W., Chen, C. H., Chang, T. W., Wu, J. M., Hwang, J. C., … Lin, Z. H. (2016). Protein-based contact electrification and its uses for mechanical energy harvesting and humidity detecting. *Nano Energy, 21*, 238–246. https://doi.org/10.1016/j.nanoen.2016.01.017

Chen, A., Zhang, C., Zhu, G., & Wang, Z. L. (2020). Polymer materials for high-performance triboelectric nanogenerators. *Advanced Science, 7*(14), Article 2000186. https://doi.org/10.1002/advs.202000186

Chen, J., Yang, J., Li, Z., Fan, X., Zi, Y., Jing, Q., … Wang, Z. L. (2015). Networks of triboelectric nanogenerators for harvesting water wave energy: A potential approach toward blue energy. *ACS Nano, 9*(3), 3324–3331. https://doi.org/10.1021/acsnano.5b00534

Chen, S., Jiang, J., Xu, F., & Gong, S. (2019). Crepe cellulose paper and nitrocellulose membrane-based triboelectric nanogenerators for energy harvesting and self-powered human-machine interaction. *Nano Energy, 61*, 69–77. https://doi.org/10.1016/j.nanoen.2019.04.043

Cui, P., Parida, K., Lin, M.-F., Xiong, J., Cai, G., & Lee, P. S. (2017). Transparent, flexible cellulose nanofibril-phosphorene hybrid paper as triboelectric nanogenerator. *Advanced Materials Interfaces, 4*(22), Article 1700651. https://doi.org/10.1002/admi.201700651

Diaz, A. F., & Felix-Navarro, R. M. (2004). A semi-quantitative tribo-electric series for polymeric materials: The influence of chemical structure and properties. *Journal of Electrostatics, 62*(4), 277–290. https://doi.org/10.1016/j.elstat.2004.05.005

Dong, L., Zheng, L., Yang, S., Yan, Z., Jin, W., & Yan, Y. (2017). Deriving freshwater safety thresholds for hexabromocyclododecane and comparison of toxicity of brominated flame retardants. *Ecotoxicology and Environmental Safety, 139*, 43–49. https://doi.org/10.1016/j.ecoenv.2017.01.005

Du, A., Zhou, B., Zhang, Z., & Shen, J. (2013). A special material or a new state of matter: A review and reconsideration of the aerogel. *Materials, 6*(3), 941–968. https://doi.org/10.3390/ma6030941

Fan, F. R., Tian, Z. Q., & Wang, Z. L. (2012). Flexible triboelectric generator. *Nano Energy, 1*(2), 328–334. https://doi.org/10.1016/j.nanoen.2012.01.004

Fang, Z., Zhu, H., Yuan, Y., Ha, D., Zhu, S., Preston, C., … Hu, L. (2014). Novel nanostructured paper with ultrahigh transparency and ultrahigh haze for solar cells. *Nano Letters, 14*(2), 765–773. https://doi.org/10.1021/nl404101p

Ghosh, S., Calizo, I., Teweldebrhan, D., Pokatilov, E. P., Nika, D. L., Balandin, A. A., … Lau, C. N. (2008). Extremely high thermal conductivity of graphene: Prospects for thermal management applications in nanoelectronic circuits. *Applied Physics Letters, 92*(15), Article 151911. https://doi.org/10.1063/1.2907977

Gong, Y., Yang, Z., Shan, X., Sun, Y., Xie, T., & Zi, Y. (2019). Capturing flow energy from ocean and wind. *Energies, 12*(11), 2184. https://doi.org/10.3390/en12112184

Han, J., Lei, T., & Wu, Q. (2014). High-water-content mouldable polyvinyl alcohol-borax hydrogels reinforced by well-dispersed cellulose nanoparticles: Dynamic rheological properties and hydrogel formation mechanism. *Carbohydrate Polymers, 102*(1), 306–316. https://doi.org/10.1016/j.carbpol.2013.11.045

Han, M., Zhang, X. S., Meng, B., Liu, W., Tang, W., Sun, X., … Zhang, H. (2013). R-shaped hybrid nanogenerator with enhanced piezoelectricity. *ACS Nano, 7*(10), 8554–8560. https://doi.org/10.1021/nn404023v

Hänninen, A., Rajala, S., Salpavaara, T., Kellomäki, M., & Tuukkanen, S. (2016). Piezoelectric sensitivity of a layered film of chitosan and cellulose nanocrystals. *Procedia Engineering, 168*, 1176–1179. https://doi.org/10.1016/j.proeng.2016.11.397

Hänninen, A., Sarlin, E., Lyyra, I., Salpavaara, T., Kellomäki, M., & Tuukkanen, S. (2018). Nanocellulose and chitosan based films as low cost, green piezoelectric materials. *Carbohydrate Polymers, 202*, 418–424. https://doi.org/10.1016/j.carbpol.2018.09.001

Hao, S., Jiao, J., Chen, Y., Wang, Z. L., & Cao, X. (2020). Natural wood-based triboelectric nanogenerator as self-powered sensing for smart homes and floors. *Nano Energy, 75*, Article 104957. https://doi.org/10.1016/j.nanoen.2020.104957

Harper, W. R. (1957). The generation of static charge. *Advances in Physics, 6*(24), 365–417. https://doi.org/10.1080/00018735700101396

He, C., Zhu, W., Chen, B., Xu, L., Jiang, T., Han, C. B., … Wang, Z. L. (2017). Smart floor with integrated triboelectric nanogenerator as energy harvester and motion sensor. *ACS Applied Materials & Interfaces, 9*(31), 26126–26133. https://doi.org/10.1021/acsami.7b08526

He, X., Zou, H., Geng, Z., Wang, X., Ding, W., Hu, F., … Wang, Z. L. (2018). A hierarchically nanostructured cellulose fiber-based triboelectric nanogenerator for self-powered healthcare products. *Advanced Functional Materials, 28*(45), Article 1805540. https://doi.org/10.1002/adfm.201805540

Hosseini, N. R., & Lee, J. S. (2015). Biocompatible and flexible chitosan-based resistive switching memory with magnesium electrodes. *Advanced Functional Materials, 25*(35), 5586–5592. https://doi.org/10.1002/adfm.201502592

Hou, T. C., Yang, Y., Zhang, H., Chen, J., Chen, L. J., & Wang, Z. L. (2013). Triboelectric nanogenerator built inside shoe insole for harvesting walking energy. *Nano Energy, 2*(5), 856–862. https://doi.org/10.1016/j.nanoen.2013.03.001

Huang, T., Wang, C., Yu, H., Wang, H., Zhang, Q., & Zhu, M. (2014). Human walking-driven wearable all-fiber triboelectric nanogenerator containing electrospun polyvinylidene fluoride piezoelectric nanofibers. *Nano Energy, 14*, 226–235. https://doi.org/10.1016/j.nanoen.2015.01.038

Jakmuangpak, S., Prada, T., Mongkolthanaruk, W., Harnchana, V., & Pinitsoontorn, S. (2020). Engineering bacterial cellulose films by nanocomposite approach and surface modification for biocompatible triboelectric nanogenerator. *ACS Applied Electronic Materials*. https://doi.org/10.1021/acsaelm.0c00421

Jang, D., Kim, Y., Kim, T. Y., Koh, K., Jeong, U., & Cho, J. (2016). Force-assembled triboelectric nanogenerator with high-humidity-resistant electricity generation using hierarchical surface morphology. *Nano Energy, 20*, 283–293. https://doi.org/10.1016/j.nanoen.2015.12.021

Jao, Y. T., Yang, P. K., Chiu, C. M., Lin, Y. J., Chen, S. W., Choi, D., … Lin, Z. H. (2018). A textile-based triboelectric nanogenerator with humidity-resistant output characteristic and its applications in self-powered healthcare sensors. *Nano Energy, 50*, 513–520. https://doi.org/10.1016/j.nanoen.2018.05.071

Jeon, J. H., Oh, I. K., Kee, C. D., & Kim, S. J. (2010). Bacterial cellulose actuator with electrically driven bending deformation in hydrated condition. *Sensors and Actuators, B: Chemical, 146*(1), 307–313. https://doi.org/10.1016/j.snb.2010.02.046

Jiang, W., Li, H., Liu, Z., Tian, J., Shi, B., … Li, Z. (2018). Fully bioabsorbable natural-materials-Based triboelectric nanogenerators. *Advanced Materials, 30*(32). https://doi.org/10.1002/adma.201801895

Jing, X., Li, H., Mi, H. Y., Feng, P. Y., Tao, X., Liu, Y., … Shen, C. (2020). Enhancing the performance of a stretchable and transparent triboelectric nanogenerator by optimizing the hydrogel ionic electrode property. *ACS Applied Materials & Interfaces, 12*(20), 23474–23483. https://doi.org/10.1021/acsami.0c04219

Jung, Y. H., Chang, T. H., Zhang, H., Yao, C., Zheng, Q., Yang, V. W., … Ma, Z. (2015). High-performance green flexible electronics based on biodegradable cellulose nanofibril paper. *Nature Communications, 6*(1), 1–11. https://doi.org/10.1038/ncomms8170

Ke, D., Liu, S., Dai, K., Zhou, J., Zhang, L., & Peng, T. (2009). CdS/regenerated cellulose nanocomposite films for highly efficient photocatalytic H2 production under visible light irradiation. *Journal of Physical Chemistry C, 113*(36), 16021–16026. https://doi.org/10.1021/jp903378q

Khandelwal, G., Maria Joseph Raj, N. P., & Kim, S. J. (2020). Triboelectric nanogenerator for healthcare and biomedical applications. *Nano Today, 33*. https://doi.org/10.1016/j.nantod.2020.100882. p. 100882.

Kim, I., Jeon, H., Kim, D., You, J., & Kim, D. (2018). All-in-one cellulose based triboelectric nanogenerator for electronic paper using simple filtration process. *Nano Energy, 53*, 975–981. https://doi.org/10.1016/j.nanoen.2018.09.060

Kim, K. N., Chun, J., Kim, J. W., Lee, K. Y., Park, J. U., Kim, S. W., … Baik, J. M. (2015). Highly stretchable 2D fabrics for wearable triboelectric nanogenerator under harsh environments. *ACS Nano, 9*(6), 6394–6400. https://doi.org/10.1021/acsnano.5b02010

Kim, M. K., Kim, M. S., Kwon, H. B., Jo, S. E., & Kim, Y. J. (2017). Wearable triboelectric nanogenerator using a plasma-etched PDMS-CNT composite for a physical activity sensor. *RSC Advances, 7*(76), 48368–48373. https://doi.org/10.1039/c7ra07623a

Kim, J. N., Lee, J., Go, T. W., Rajabi-Abhari, A., Mahato, M., Park, J. Y., … Oh, I. K. (2020). Skin-attachable and biofriendly chitosan-diatom triboelectric nanogenerator. *Nano Energy, 75*, Article 104904. https://doi.org/10.1016/j.nanoen.2020.104904

Kim, D. W., Lee, J. H., Kim, J. K., & Jeong, U. (2020). Material aspects of triboelectric energy generation and sensors. *NPG Asia Materials, 12*, 1–17. https://doi.org/10.1038/s41427-019-0176-0

Kim, H. J., Yim, E. C., Kim, J. H., Kim, S. J., Park, J. Y., & Oh, I. K. (2017). Bacterial nanocellulose triboelectric nanogenerator. *Nano Energy, 33*, 130–137. https://doi.org/10.1016/j.nanoen.2017.01.035

Klemm, D., Kramer, F., Moritz, S., Lindström, T., Ankerfors, M., Gray, D., … Dorris, A. (2011). Nanocelluloses: A new family of nature-based materials. *Angewandte Chemie - International Edition, 50*(24), 5438–5466. https://doi.org/10.1002/anie.201001273

Kumar, R., Ranwa, S., & Kumar, G. (2020). Biodegradable flexible substrate based on chitosan/PVP blend polymer for disposable electronics device applications. *The Journal of Physical Chemistry B, 124*(1), 149–155. https://doi.org/10.1021/acs.jpcb.9b08897

Kwon, K. Y., Lee, J. S., Ko, G. J., Sunwoo, S. H., Lee, S., Jo, Y. J., … il Kim, T. (2018). Biosafe, eco-friendly levan polysaccharide toward transient electronics. *Small, 14*(32), Article 1801332. https://doi.org/10.1002/smll.201801332

Lacks, D. J., & Mohan Sankaran, R. (2011). Contact electrification of insulating materials. *Journal of Physics D: Applied Physics, 44*(45). https://doi.org/10.1088/0022-3727/44/45/453001, 453001.

Lee, I., & Lee, K. (2015). The Internet of Things (IoT): Applications, investments, and challenges for enterprises. *Business Horizons, 58*(4), 431–440. https://doi.org/10.1016/j.bushor.2015.03.008

Lee, B. Y., Kim, D. H., Park, J., Park, K. I., Lee, K. J., & Jeong, C. K. (2019). Modulation of surface physics and chemistry in triboelectric energy harvesting technologies. *Science and Technology of Advanced Materials, 20*(1), 758–773. https://doi.org/10.1080/14686996.2019.1631716

Lee, K. Y., Chun, J., Lee, J. H., Kim, K. N., Kang, N. R., Kim, J. Y., … Kim, S. W. (2014). Hydrophobic sponge structure-based triboelectric nanogenerator. *Advanced Materials, 26*(29), 5037–5042. https://doi.org/10.1002/adma.201401184

Lee, S., Wang, H., Shi, Q., Dhakar, L., Wang, J., Thakor, N. V., … Lee, C. (2017). Development of battery-free neural interface and modulated control of tibialis anterior muscle via common peroneal nerve based on triboelectric nanogenerators (TENGs). *Nano Energy, 33*, 1–11. https://doi.org/10.1016/j.nanoen.2016.12.038

Li, L., Zhang, H., Cao, H., Zhang, L., Liang, L., Gao, J., … Zhou, J. (2016). Proton conducting sodium-alginate-gated oxide thin-film transistors with varying device structure. *Physica Status Solidi (A), 213*(12), 3103–3109. https://doi.org/10.1002/pssa.201600214

Li, X., Ding, C., Li, X., Yang, H., Liu, S., Wang, X., … Chen, J. (2020). October). Electronic biopolymers: From molecular engineering to functional devices. *Chemical Engineering Journal, 397*. https://doi.org/10.1016/j.cej.2020.125499. p. 125499.

Li, X., Shu, M., Li, H., Gao, X., Long, S., Hu, T., … Wu, C. (2018). Strong, tough and mechanically self-recoverable poly(vinyl alcohol)/alginate dual-physical double-network hydrogels with large cross-link density contrast. *RSC Advances, 8*(30), 16674–16689. https://doi.org/10.1039/c8ra01302k

Li, Z., Shen, J., Abdalla, I., Yu, J., & Ding, B. (2017). Nanofibrous membrane constructed wearable triboelectric nanogenerator for high performance biomechanical energy harvesting. *Nano Energy, 36*, 341–348. https://doi.org/10.1016/j.nanoen.2017.04.035

Liang, Q., Zhang, Q., Yan, X., Liao, X., Han, L., Yi, F., … Zhang, Y. (2017). Recyclable and green triboelectric nanogenerator. *Advanced Materials, 29*(5), Article 1604961. https://doi.org/10.1002/adma.201604961

Lin, L., Wang, S., Xie, Y., Jing, Q., Niu, S., Hu, Y., … Wang, Z. L. (2013). Segmentally structured disk triboelectric nanogenerator for harvesting rotational mechanical energy. *Nano Letters, 13*(6), 2916–2923. https://doi.org/10.1021/nl4013002

Lithner, D., Larsson, A., & Dave, G. (2011). Environmental and health hazard ranking and assessment of plastic polymers based on chemical composition. *The Science of the Total Environment, 409*(18), 3309–3324. https://doi.org/10.1016/j.scitotenv.2011.04.038

Liu, H., Zhong, J., Lee, C., Lee, S. W., & Lin, L. (2018). A comprehensive review on piezoelectric energy harvesting technology: Materials, mechanisms, and applications. *Applied Physics Reviews, 5*(4), 41306. https://doi.org/10.1063/1.5074184

Lu, Y., Li, X., Ping, J., He, J., & Wu, J. (2020). A flexible, recyclable, and high-performance pullulan-based triboelectric nanogenerator (TENG). *Advanced Materials & Technologies, 5*(2), Article 1900905. https://doi.org/10.1002/admt.201900905

Luo, J., Wang, Z., Xu, L., Wang, A. C., Han, K., Jiang, T., … Wang, Z. L. (2019). Flexible and durable wood-based triboelectric nanogenerators for self-powered sensing in athletic big data analytics. *Nature Communications, 10*(1), 1–9. https://doi.org/10.1038/s41467-019-13166-6

Ma, C., Gao, S., Gao, X., Wu, M., Wang, R., Wang, Y., … Wu, W. (2019). Chitosan biopolymer-derived self-powered triboelectric sensor with optimized performance through molecular surface engineering and data-driven learning. *InfoMat, 1*(1), 116–125. https://doi.org/10.1002/inf2.12008

Ma, M., Kang, Z., Liao, Q., Zhang, Q., Gao, F., Zhao, X., … Zhang, Y. (2018). Development, applications, and future directions of triboelectric nanogenerators. *Nano Research, 11*(6), 2951–2969. https://doi.org/10.1007/s12274-018-1997-9

Maiti, S., Karan, S. K., Kim, J. K., & Khatua, B. B. (2019). Nature driven bio-piezoelectric/triboelectric nanogenerator as next-generation green energy harvester for smart and pollution free society. *Advanced Energy Materials, 9*(9), Article 1803027. https://doi.org/10.1002/aenm.201803027

Mangayil, R., Rajala, S., Pammo, A., Sarlin, E., Luo, J., Santala, V., … Tuukkanen, S. (2017). Engineering and characterization of bacterial nanocellulose films as low cost and flexible sensor material. *ACS Applied Materials & Interfaces, 9*(22), 19048–19056. https://doi.org/10.1021/acsami.7b04927

McCarty, L. S., & Whitesides, G. M. (2008). Electrostatic charging due to separation of ions at interfaces: Contact electrification of ionic electrets. *Angewandte Chemie – International Edition, 47*(12), 2188–2207. https://doi.org/10.1002/anie.200701812

Meng, X., Yang, J., Liu, Z., Lu, W., Sun, Y., & Dai, Y. (2020). Non-contact, fibrous cellulose acetate/aluminum flexible electronic-sensor for humidity detecting. *Composites Communications, 20*, Article 100347. https://doi.org/10.1016/j.coco.2020.04.013

Mi, H. Y., Jing, X., Zheng, Q., Fang, L., Huang, H. X., Turng, L. S., … Gong, S. (2018). High-performance flexible triboelectric nanogenerator based on porous aerogels and electrospun nanofibers for energy harvesting and sensitive self-powered sensing. *Nano Energy, 48*, 327–336. https://doi.org/10.1016/j.nanoen.2018.03.050

Miao, J., Liu, H., Li, Y., & Zhang, X. (2018). Biodegradable transparent substrate based on edible starch-chitosan embedded with nature-inspired three-dimensionally interconnected conductive nanocomposites for wearable green electronics. *ACS Applied Materials & Interfaces, 10*(27), 23037–23047. https://doi.org/10.1021/acsami.8b04291

Narita, F., & Fox, M. (2018). A review on piezoelectric, magnetostrictive, and magnetoelectric materials and device technologies for energy harvesting applications. *Advanced Engineering Materials, 20*(5), Article 1700743. https://doi.org/10.1002/adem.201700743

Needhidasan, S., Samuel, M., & Chidambaram, R. (2014). Electronic waste - an emerging threat to the environment of urban India. *Journal of Environmental Health Science & Engineering, 12*(1), 1–9. https://doi.org/10.1186/2052-336X-12-36

Niu, S., Liu, Y., Chen, X., Wang, S., Zhou, Y. S., Lin, L., … Wang, Z. L. (2015). Theory of freestanding triboelectric-layer-based nanogenerators. *Nano Energy, 12*, 760–774. https://doi.org/10.1016/j.nanoen.2015.01.013

Niu, S., Liu, Y., Wang, S., Lin, L., Zhou, Y. S., Hu, Y., … Wang, Z. L. (2014). Theoretical investigation and structural optimization of single-electrode triboelectric nanogenerators. *Advanced Functional Materials, 24*(22), 3332–3340. https://doi.org/10.1002/adfm.201303799

Niu, S., Liu, Y., Wang, S., Lin, L., Zhou, Y. S., Hu, Y., … Wang, Z. L. (2013). Theory of sliding-mode triboelectric nanogenerators. *Advanced Materials, 25*(43), 6184–6193. https://doi.org/10.1002/adma.201302808

Niu, S., Wang, S., Lin, L., Liu, Y., Zhou, Y. S., Hu, Y., … Wang, Z. L. (2013). Theoretical study of contact-mode triboelectric nanogenerators as an effective power source. *Energy & Environmental Science, 6*(12), 3576–3583. https://doi.org/10.1039/c3ee42571a

Nye, J. F. (1957). *Physical properties of crystals*. Oxford: The Charendon Press.

Oh, H., Kwak, S. S., Kim, B., Han, E., Lim, G., Kim, S., … Lim, B. (2019). Highly conductive ferroelectric cellulose composite papers for efficient triboelectric nanogenerators. *Advanced Functional Materials, 29*(37), Article 1904066. https://doi.org/10.1002/adfm.201904066

Pan, R., Xuan, W., Chen, J., Dong, S., Jin, H., Wang, X., … Luo, J. (2018). Fully biodegradable triboelectric nanogenerators based on electrospun polylactic acid and nanostructured gelatin films. *Nano Energy, 45*, 193–202. https://doi.org/10.1016/j.nanoen.2017.12.048

Pandey, A. R., Singh, U. S., Momin, M., & Bhavsar, C. (2017). Chitosan: Application in tissue engineering and skin grafting. *Journal of Polymer Research, 24*(8), 1–22. https://doi.org/10.1007/s10965-017-1286-4

Pang, Y., Xi, F., Luo, J., Liu, G., Guo, T., & Zhang, C. (2018). An alginate film-based degradable triboelectric nanogenerator. *RSC Advances, 8*(12), 6719–6726. https://doi.org/10.1039/c7ra13294h

Parandeh, S., Kharaziha, M., & Karimzadeh, F. (2019). An eco-friendly triboelectric hybrid nanogenerators based on graphene oxide incorporated polycaprolactone fibers and cellulose paper. *Nano Energy, 59*, 412–421. https://doi.org/10.1016/j.nanoen.2019.02.058

Peng, J., Zhang, H., Zheng, Q., Clemons, C. M., Sabo, R. C., Gong, S., … Turng, L. S. (2017). A composite generator film impregnated with cellulose nanocrystals for enhanced triboelectric performance. *Nanoscale, 9*(4), 1428–1433. https://doi.org/10.1039/c6nr07602e

Qian, C., Li, L., Gao, M., Yang, H., Cai, Z., Chen, B., … Song, Y. (2019). All-printed 3D hierarchically structured cellulose aerogel based triboelectric nanogenerator for multi-functional sensors. *Nano Energy, 63*, Article 103885. https://doi.org/10.1016/j.nanoen.2019.103885

Quan, Z., Han, C. B., Jiang, T., & Wang, Z. L. (2016). Robust thin films-based triboelectric nanogenerator arrays for harvesting bidirectional wind energy. *Advanced Energy Materials, 6*(5), Article 1501799. https://doi.org/10.1002/aenm.201501799

Rajala, S., Siponkoski, T., Sarlin, E., Mettänen, M., Vuoriluoto, M., Pammo, A., … Tuukkanen, S. (2016). Cellulose nanofibril film as a piezoelectric sensor material. *ACS Applied Materials & Interfaces, 8*(24), 15607–15614. https://doi.org/10.1021/acsami.6b03597

Roy, S., Ko, H. U., Maji, P. K., Van Hai, L., & Kim, J. (2020). Large amplification of triboelectric property by allicin to develop high performance cellulosic triboelectric

nanogenerator. *Chemical Engineering Journal, 385*, Article 123723. https://doi.org/10.1016/j.cej.2019.123723
Ryu, H., Lee, J., Kim, T.-Y., Khan, U., Lee, J. H., Kwak, S. S., … Kim, S. W. (2017). High-performance triboelectric nanogenerators based on solid polymer electrolytes with asymmetric pairing of ions. *Advanced Energy Materials, 7*(17), Article 1700289. https://doi.org/10.1002/aenm.201700289
Saadatnia, Z., Esmailzadeh, E., & Naguib, H. E. (2019). High performance triboelectric nanogenerator by hot embossing on self-assembled micro-particles. *Advanced Engineering Materials, 21*(1), Article 1700957. https://doi.org/10.1002/adem.201700957
Sadasivuni, K. K., Kafy, A., Kim, H. C., Ko, H. U., Mun, S., & Kim, J. (2015). Reduced graphene oxide filled cellulose films for flexible temperature sensor application. *Synthetic Metals, 206*, 154–161. https://doi.org/10.1016/j.synthmet.2015.05.018
Sarkar, P. K., Kamilya, T., & Acharya, S. (2019). Introduction of triboelectric positive bioplastic for powering portable electronics and self-powered gait sensor. *ACS Applied Energy Materials, 2*(8), 5507–5514. https://doi.org/10.1021/acsaem.9b00677
Shao, Y., ping Feng, C., wen Deng, B., Yin, B., & bo Yang, M. (2019). Facile method to enhance output performance of bacterial cellulose nanofiber based triboelectric nanogenerator by controlling micro-nano structure and dielectric constant. *Nano Energy, 62*, 620–627. https://doi.org/10.1016/j.nanoen.2019.05.078
Shi, M., & Wu, H. (2019). Applications in internet of things and artificial intelligence. *Flexible and stretchable triboelectric nanogenerator devices* (pp. 359–378). https://doi.org/10.1002/9783527820153.ch18
Shi, X., Chen, S., Zhang, H., Jiang, J., Ma, Z., & Gong, S. (2019). Portable self-charging power system via integration of a flexible paper-based triboelectric nanogenerator and supercapacitor. *ACS Sustainable Chemistry & Engineering, 7*(22), 18657–18666. https://doi.org/10.1021/acssuschemeng.9b05129
Shi, K., Huang, X., Sun, B., Wu, Z., He, J., & Jiang, P. (2019). Cellulose/BaTiO 3 aerogel paper based flexible piezoelectric nanogenerators and the electric coupling with triboelectricity. *Nano Energy, 57*, 450–458. https://doi.org/10.1016/j.nanoen.2018.12.076
Song, G., Kim, Y., Yu, S., Kim, M. O., Park, S. H., Cho, S. M., … Park, C. (2015). Molecularly engineered surface triboelectric nanogenerator by self-assembled monolayers (METS). *Chemistry of Materials, 27*(13), 4749–4755. https://doi.org/10.1021/acs.chemmater.5b01507
Song, P., Kuang, S., Panwar, N., Yang, G., Tng, D. J. H., Tjin, S. C., … Wang, Z. L. (2017). A self-powered implantable drug-delivery system using biokinetic energy. *Advanced Materials, 29*(11), Article 1605668. https://doi.org/10.1002/adma.201605668
Sriphan, S., & Vittayakorn, N. (2018). Facile roughness fabrications and their roughness effects on electrical outputs of the triboelectric nanogenerator. *Smart Materials & Structures, 27*(10), 105026. https://doi.org/10.1088/1361-665X/AADB65
Sriplai, N., Mangayil, R., Pammo, A., Santala, V., Tuukkanen, S., & Pinitsoontorn, S. (2020). Enhancing piezoelectric properties of bacterial cellulose films by incorporation of MnFe2O4 nanoparticles. *Carbohydrate Polymers, 231*, Article 115730. https://doi.org/10.1016/j.carbpol.2019.115730
Srither, S. R., Shankar Rao, D. S., & Krishna Prasad, S. (2018). Triboelectric nanogenerator based on biocompatible and easily available polymer films. *ChemistrySelect, 3*(18), 5055–5061. https://doi.org/10.1002/slct.201800685
Sun, Y., Zeng, K. Y., & Li, T. (2020). Piezo-/ferroelectric phenomena in biomaterials: A brief review of recent progress and perspectives. *Science China: Physics, Mechanics and Astronomy, 63*(7), 278701. https://doi.org/10.1007/s11433-019-1500-y
Šutka, A., Ruža, J., Järvekülg, M., Linarts, A., Mālnieks, K., Jurķāns, V., … Knite, M. (2018). Triboelectric nanogenerator based on immersion precipitation derived highly porous ethyl cellulose. *Journal of Electrostatics, 92*, 1–5. https://doi.org/10.1016/j.elstat.2018.01.003
Tanskanen, P. (2013). Management and recycling of electronic waste. *Acta Materialia, 61*(3), 1001–1011. https://doi.org/10.1016/j.actamat.2012.11.005
Tian, J., Shi, R., Liu, Z., Ouyang, H., Yu, M., Zhao, C., … Li, Z. (2019). Self-powered implantable electrical stimulator for osteoblasts' proliferation and differentiation. *Nano Energy, 59*, 705–714. https://doi.org/10.1016/j.nanoen.2019.02.073
Tian, J., Chen, X., & Wang, Z. L. (2020). Environmental energy harvesting based on triboelectric nanogenerators. *Nanotechnology, 31*(24), Article 242001. https://doi.org/10.1088/1361-6528/AB793E
Torres, F. G., Arroyo, J., Alvarez, R., Rodriguez, S., Troncoso, O., & López, D. (2019). Carboxymethyl κ/ι-hybrid carrageenan doped with NH4I as a template for solid bio-electrolytes development. *Materials Chemistry and Physics, 223*, 659–665. https://doi.org/10.1016/j.matchemphys.2018.11.051
Torres, F. G., Arroyo, J. J., & Troncoso, O. P. (2019). Bacterial cellulose nanocomposites: An all-nano type of material. *Materials Science and Engineering C, 98*, 1277–1293. https://doi.org/10.1016/j.msec.2019.01.064
Trache, D., Hussin, M. H., Hui Chuin, C. T., Sabar, S., Fazita, M. R. N., Taiwo, O. F. A., … Haafiz, M. K. M. (2016). Microcrystalline cellulose: Isolation, characterization and bio-composites application—A review. *International Journal of Biological Macromolecules, 93*, 789–804. https://doi.org/10.1016/j.ijbiomac.2016.09.056
Tuukkanen, S., & Rajala, S. (2018). Nanocellulose as a piezoelectric material. *Piezoelectricity - organic and inorganic materials and applications*. https://doi.org/10.5772/intechopen.77025
Uddin, A. S. M. I., & Chung, G. S. (2017). Wide-ranging impact-competent self-powered active sensor using a stacked corrugated-core sandwich-structured robust triboelectric nanogenerator. *Sensors and Actuators, B: Chemical, 245*, 1–10. https://doi.org/10.1016/j.snb.2017.01.111
Vivekananthan, V., Chandrasekhar, A., Alluri, N. R., Purusothaman, Y., & Kim, S.-J. (2020). A highly reliable, impervious and sustainable triboelectric nanogenerator as a zero-power consuming active pressure sensor. *Nanoscale Advances, 2*(2), 746–754. https://doi.org/10.1039/c9na00790c
Wang, Z. L. (2013). Triboelectric nanogenerators as new energy technology for self-powered systems and as active mechanical and chemical sensors. *ACS Nano, 7*(11), 9533–9557. https://doi.org/10.1021/nn404614z
Wang, Z. L. (2014). Triboelectric nanogenerators as new energy technology and self-powered sensors - Principles, problems and perspectives. *Faraday Discussions, 176*, 447–458. https://doi.org/10.1039/c4fd00159a
Wang, Z. L. (2020a). Triboelectric nanogenerator (TENG)—Sparking an energy and sensor revolution. *Advanced Energy Materials, 10*(17), Article 2000137. https://doi.org/10.1002/aenm.202000137
Wang, Z. L. (2020b). On the first principle theory of nanogenerators from Maxwell's equations. *Nano Energy, 68*, Article 104272. https://doi.org/10.1016/j.nanoen.2019.104272
Wang, L., & Daoud, W. A. (2019). Hybrid conductive hydrogels for washable human motion energy harvester and self-powered temperature-stress dual sensor. *Nano Energy, 66*, Article 104080. https://doi.org/10.1016/j.nanoen.2019.104080
Wang, J., Tavakoli, J., & Tang, Y. (2019). Bacterial cellulose production, properties and applications with different culture methods – A review. *Carbohydrate Polymers, 219*, 63–76. https://doi.org/10.1016/j.carbpol.2019.05.008
Wang, M., Li, W., You, C., Wang, Q., Zeng, X., & Chen, M. (2017). Triboelectric nanogenerator based on 317L stainless steel and ethyl cellulose for biomedical applications. *RSC Advances, 7*(11), 6772–6779. https://doi.org/10.1039/c6ra28252k
Wang, R., Gao, S., Yang, Z., Li, Y., Chen, W., Wu, B., … Wu, W. (2018). Engineered and laser-processed chitosan biopolymers for sustainable and biodegradable triboelectric power generation. *Advanced Materials, 30*(11), Article 1706267. https://doi.org/10.1002/adma.201706267
Wang, S., Lin, L., & Wang, Z. L. (2012). Nanoscale triboelectric-effect-enabled energy conversion for sustainably powering portable electronics. *Nano Letters, 12*(12), 6339–6346. https://doi.org/10.1021/nl303573d
Wang, S., Lin, L., Xie, Y., Jing, Q., Niu, S., & Wang, Z. L. (2013). Sliding-triboelectric nanogenerators based on in-plane charge-separation mechanism. *Nano Letters, 13*(5), 2226–2233. https://doi.org/10.1021/nl400738p
Wang, W., Lin, J., Cheng, J., Cui, Z., Si, J., Wang, Q., … Turng, L. S. (2020). Dual super-amphiphilic modified cellulose acetate nanofiber membranes with highly efficient oil/water separation and excellent antifouling properties. *Journal of Hazardous Materials, 385*, Article 121582. https://doi.org/10.1016/j.jhazmat.2019.121582
Wang, Z. L., Lin, L., Chen, J., Niu, S., & Zi, Y. (2016). *Triboelectric nanogenerator: Freestanding triboelectric-layer mode*. https://doi.org/10.1007/978-3-319-40039-6_5
Wang, S., Mu, X., Wang, X., Gu, A. Y., Wang, Z. L., & Yang, Y. (2015). Elasto-aerodynamics-driven triboelectric nanogenerator for scavenging air-flow energy. *ACS Nano, 9*(10), 9554–9563. https://doi.org/10.1021/acsnano.5b04396
Wang, X., Niu, S., Yin, Y., Yi, F., You, Z., & Wang, Z. L. (2015). Triboelectric nanogenerator based on fully enclosed rolling spherical structure for harvesting low-frequency water wave energy. *Advanced Energy Materials, 5*(24). https://doi.org/10.1002/aenm.201501467
Wang, S., Xie, Y., Niu, S., Lin, L., Liu, C., Zhou, Y. S., … Wang, Z. L. (2014). Maximum surface charge density for triboelectric nanogenerators achieved by ionized-air injection: Methodology and theoretical understanding. *Advanced Materials, 26*(39), 6720–6728. https://doi.org/10.1002/adma.201402491
Wang, S., Xie, Y., Niu, S., Lin, L., & Wang, Z. L. (2014). Freestanding triboelectric-layer-based nanogenerators for harvesting energy from a moving object or human motion in contact and non-contact modes. *Advanced Materials, 26*(18), 2818–2824. https://doi.org/10.1002/adma.201305303
Wei, X. Y., Zhu, G., & Wang, Z. L. (2014). Surface-charge engineering for high-performance triboelectric nanogenerator based on identical electrification materials. *Nano Energy, 10*, 83–89. https://doi.org/10.1016/j.nanoen.2014.08.007
Wu, C., Wang, A. C., Ding, W., Guo, H., & Wang, Z. L. (2019). Triboelectric nanogenerator: A foundation of the energy for the new era. *Advanced Energy Materials, 9*. https://doi.org/10.1002/aenm.201802906
Yang, B., Lee, C., Xiang, W., Xie, J., Han He, J., Kotlanka, R. K., … Feng, H. (2009). Electromagnetic energy harvesting from vibrations of multiple frequencies. *Journal of Micromechanics and Microengineering, 19*(3), 35001. https://doi.org/10.1088/0960-1317/19/3/035001
Yang, B., Yao, C., Yu, Y., Li, Z., & Wang, X. (2017). Nature degradable, flexible, and transparent conductive substrates from green and earth-abundant materials. *Scientific Reports, 7*(1), 1–8. https://doi.org/10.1038/s41598-017-04969-y
Yang, Y., Zhang, H., Chen, J., Jing, Q., Zhou, Y. S., Wen, X., … Wang, Z. L. (2013). Single-electrode-based sliding triboelectric nanogenerator for self-powered displacement vector sensor system. *ACS Nano, 7*(8), 7342–7351. https://doi.org/10.1021/nn403021m
Yang, Y., Zhou, Y. S., Zhang, H., Liu, Y., Lee, S., & Wang, Z. L. (2013). A single-electrode based triboelectric nanogenerator as self-powered tracking system. *Advanced Materials, 25*(45), 6594–6601. https://doi.org/10.1002/adma.201302453
Yao, C., Hernandez, A., Yu, Y., Cai, Z., & Wang, X. (2016). Triboelectric nanogenerators and power-boards from cellulose nanofibrils and recycled materials. *Nano Energy, 30*, 103–108. https://doi.org/10.1016/j.nanoen.2016.09.036
Yao, C., Yin, X., Yu, Y., Cai, Z., & Wang, X. (2017). Chemically functionalized natural cellulose materials for effective triboelectric nanogenerator development. *Advanced Functional Materials, 27*(30), Article 1700794. https://doi.org/10.1002/adfm.201700794
Yu, A., Zhu, Y., Wang, W., & Zhai, J. (2019). Progress in triboelectric materials: Toward high performance and widespread applications. *Advanced Functional Materials, 29*(41), Article 1900098. https://doi.org/10.1002/adfm.201900098
Yu, Z., Wang, Y., Zheng, J., Xiang, Y., Zhao, P., Cui, J., … Li, D. (2020). Rapidly fabricated triboelectric nanogenerator employing insoluble and infusible biomass

materials by fused deposition modeling. *Nano Energy, 68*, Article 104382. https://doi.org/10.1016/j.nanoen.2019.104382

Zhang, L., Liao, Y., Wang, Y., Zhang, S., Yang, W., Pan, X., … Wang, Z. L. (2020). Cellulose II Aerogel-Based Triboelectric Nanogenerator. *Advanced Functional Materials*. , Article 2001763. https://doi.org/10.1002/adfm.202001763

Zhang, L., Zhang, B., Chen, J., Jin, L., Deng, W., Tang, J., … Wang, Z. L. (2016). Lawn structured triboelectric nanogenerators for scavenging sweeping wind energy on rooftops. *Advanced Materials, 28*(8), 1650–1656. https://doi.org/10.1002/adma.201504462

Zhang, C., Lin, X., Zhang, N., Lu, Y., Wu, Z., Liu, G., … Nie, S. (2019). Chemically functionalized cellulose nanofibrils-based gear-like triboelectric nanogenerator for energy harvesting and sensing. *Nano Energy, 66*, Article 104126. https://doi.org/10.1016/j.nanoen.2019.104126

Zhang, B., Tang, Y., Dai, R., Wang, H., Sun, X., Qin, C., … Mao, Y. (2019). Breath-based human–machine interaction system using triboelectric nanogenerator. *Nano Energy, 64*, Article 103953. https://doi.org/10.1016/j.nanoen.2019.103953

Zhao, D., Zhu, Y., Cheng, W., Chen, W., Wu, Y., & Yu, H. (2020). Cellulose-based flexible functional materials for emerging intelligent electronics. *Advanced Materials*. , Article 2000619. https://doi.org/10.1002/adma.202000619

Zhao, Z., Pu, X., Du, C., Li, L., Jiang, C., Hu, W., … Wang, Z. L. (2016). Freestanding flag-type triboelectric nanogenerator for harvesting high-altitude wind energy from arbitrary directions. *ACS Nano, 10*(2), 1780–1787. https://doi.org/10.1021/acsnano.5b07157

Zhao, Z., Yan, C., Liu, Z., Fu, X., Peng, L. M., Hu, Y., … Zheng, Z. (2016). Machine-washable textile triboelectric nanogenerators for effective human respiratory monitoring through loom weaving of metallic yarns. *Advanced Materials, 28*(46), 10267–10274. https://doi.org/10.1002/adma.201603679

Zhao, L., Zheng, Q., Ouyang, H., Li, H., Yan, L., Shi, B., … Li, Z. (2016). A size-unlimited surface microstructure modification method for achieving high performance triboelectric nanogenerator. *Nano Energy, 28*, 172–178. https://doi.org/10.1016/j.nanoen.2016.08.024

Zheng, Q., Shi, B., Fan, F., Wang, X., Yan, L., Yuan, W., … Wang, Z. L. (2014). In vivo powering of pacemaker by breathing-driven implanted triboelectric nanogenerator. *Advanced Materials, 26*(33), 5851–5856. https://doi.org/10.1002/adma.201402064

Zheng, Q., Zou, Y., Zhang, Y., Liu, Z., Shi, B., Wang, X., … Wang, Z. L. (2016). Biodegradable triboelectric nanogenerator as a life-time designed implantable power source. *Science Advances, 2*(3), Article e1501478. https://doi.org/10.1126/sciadv.1501478

Zheng, Q., Fang, L., Guo, H., Yang, K., Cai, Z., Meador, M. A. B., … Gong, S. (2018). Highly porous polymer aerogel film-based triboelectric nanogenerators. *Advanced Functional Materials, 28*(13), Article 1706365. https://doi.org/10.1002/adfm.201706365

Zhou, L., Liu, D., Wang, J., & Wang, Z. L. (2020). Triboelectric nanogenerators: Fundamental physics and potential applications. *Friction, 8*(3), 481–506. https://doi.org/10.1007/s40544-020-0390-3

Zhou, T., Zhang, C., Han, C. B., Fan, F. R., Tang, W., & Wang, Z. L. (2014). Woven structured triboelectric nanogenerator for wearable devices. *ACS Applied Materials & Interfaces, 6*(16), 14695–14701. https://doi.org/10.1021/am504110u

Zhu, G., Pan, C., Guo, W., Chen, C. Y., Zhou, Y., Yu, R., … Wang, Z. L. (2012). Triboelectric-generator-driven pulse electrodeposition for micropatterning. *Nano Letters, 12*(9), 4960–4965. https://doi.org/10.1021/nl302560k

Zhu, G., Peng, B., Chen, J., Jing, Q., & Wang, Z. L. (2014). Triboelectric nanogenerators as a new energy technology: From fundamentals, devices, to applications. *Nano Energy, 14*, 126–138. https://doi.org/10.1016/j.nanoen.2014.11.050

Zhu, Z., Xia, K., Xu, Z., Lou, H., & Zhang, H. (2018). Starch paper-based triboelectric nanogenerator for human perspiration sensing. *Nanoscale Research Letters, 13*(1), 365. https://doi.org/10.1186/s11671-018-2786-9

Zhu, G., Chen, J., Liu, Y., Bai, P., Zhou, Y. S., Jing, Q., … Wang, Z. L. (2013). Linear-grating triboelectric generator based on sliding electrification. *Nano Letters, 13*(5), 2282–2289. https://doi.org/10.1021/nl4008985

Zhu, H., Xiao, Z., Liu, D., Li, Y., Weadock, N. J., Fang, Z., … Hu, L. (2013). Biodegradable transparent substrates for flexible organic-light-emitting diodes. *Energy & Environmental Science, 6*(7), 2105–2111. https://doi.org/10.1039/c3ee40492g

Zong, A., Cao, H., & Wang, F. (2012). Anticancer polysaccharides from natural resources: A review of recent research. *Carbohydrate Polymers, 90*(4), 1395–1410. https://doi.org/10.1016/j.carbpol.2012.07.026

Zou, H., Zhang, Y., Guo, L., Wang, P., He, X., Dai, G., … Wang, Z. L. (2019). Quantifying the triboelectric series. *Nature Communications, 10*(1), 1–9. https://doi.org/10.1038/s41467-019-09461-x